EVALUATION OF ANTI-CORROSION AND ANTI-GALLING PERFORMANCE OF A NOVEL GREASE COMPOUND

A Thesis

by

JOHN OLUMIDE REIS

Submitted to the Office of Graduate and Professional Studies of
Texas A&M University
in partial fulfillment of the requirements for the degree of

MASTER OF SCIENCE

Chair of Committee,	Hong Liang
Committee Members,	Chii-Der Suh
	Sevan Goenezan
Head of Department,	Andreas A. Polycarpou

December 2017

Major Subject: Mechanical Engineering

ABSTRACT

In this research, the effectiveness of CeO2, Y2O3 and Al2O3 as anti-corrosion and anti-wear additives in commercial grease was investigated. An experimental approach was used to carry on the research. The weight loss of steel coupons protected with a layer of thin grease, with and without the anti-corrosion additives in a corrosive environment was determined. The Friction factor of the grease compound was also evaluated.

The accelerated corrosion tests were performed in a salt spray chamber for an exposure time of 2 weeks (336 hours). The corrosive medium was 5 % wt. of Brine. By varying the weight compositions of the additives (1% wt. and 3% wt.), and comparing the corrosion rates with that of base grease, the effectiveness of various grease additives was evaluated. The result showed that corrosive losses of the test samples can be effectively reduced by adding relatively small amounts of CeO_2, Y_2O_3 and Al_2O_3 to the base grease. Corroded surfaces were examined using the Optical microscope to clarify the corrosion mechanism.

The friction test was carried out using a galling tester. The standard test procedure as specified in API RP 7A1 was followed. The result showed that frictional performance of thread compounds can be improved by adding small amounts (1% wt. – 3% wt.) of Y_2O_3 and Al_2O_3 as additives.

DEDICATION

This thesis is dedicated to my parents and my significant other, who have so patiently steered and supported my ambitions. All of it will count for good.

ACKNOWLEDGEMENTS

First, I give thanks to God for seeing me through. He has been my help every step of the way.

I would also like to express my profound gratitude to my advisor, Dr. Liang. Her guidance and advice has steered this work to its successful completion.

Furthermore, I would like to show my appreciation Dr. Suh, Dr. Goenezen and Dr. Mukherjee, for kindly and openhandedly accepting to be my committee members despite their busy schedule.

I am deeply indebted to all members of the surface science group for the valuable suggestions, critique and support. Particularly Dr Carlos Sanchez, Dr. Wei Dai and Lian Ma.

Finally, I would like to acknowledge with much appreciation the crucial role of Dr. Homero Castaneda of the materials science & engineering department for his invaluable suggestion and contribution to this work. He helped overcome a fundamental challenge in this work.

CONTRIBUTORS AND FUNDING SOURCES

Contributors

This work was supervised by a thesis committee consisting of Professor Hong Liang, Professor Steve Suh and Professor Sevan Goenezan of the Department of Mechanical Engineering.

Dr. Carlos Sanchez, Wei Dai, and Lian Ma Provided sample materials. The facility to evaluate corrosion and galling was supported by the Department of Mechanical Engineering, Texas A&M University.

Funding Sources

This work was in part supported by Schlumberger, Bestolife, and Texas A&M University Strategic Seed Grant Program.

NOMENCLATURE

μ	Coefficient of friction
S_1	Average slope of the first 8 runs of reference compound
S_2	Average slope of the 8 runs of test thread compound
S_3	Average slope of the second 8 runs of reference compound
Std.Dev.	Standard Deviation
ASTM	American Society for Testing and Materials
B/O	Break out
M/U	Make up
COF	Coefficient of Friction
FF	Friction factor
NLGI	National Lubricating Grease Institute.
UCF	Upper Curve Fit
LCF	Lower Curve Fit

TABLE OF CONTENTS

LIST OF FIGURES

LIST OF TABLES

CHAPTER I

INTRODUCTION

Material losses due to poor lubrication can be in the form of corrosive losses or material losses due to wear (galling). In this research, the effectiveness of some oxide additives (CeO_2, Y_2O_3 and Al_2O_3) in lubricating grease was evaluated on the basis of corrosion protection and anti-galling performance.

This chapter provides a brief background into this research. It provides understanding of fundamental concepts discussed in subsequent chapters.

1.1 Economic Impact of Corrosion

Material losses in the form of corrosion costs not just money but also lives. Corrosion results in unplanned failures and rising cost for everything including, services, transportation and a lot more. According to Generation 2 Material Technology (GM2T) labs, the projected cost of corrosion to the US economy in 2016 was $1.1 trillion, and this is money going down the drain. Losses as a result of corrosion grosses over 6.2% of the GDP, and this remains one of the largest single expenses in the US economy yet it largely remains unattended [1]. A broader application of best practices and corrosion resistant materials could approximately reduce one-third of these cost [2].

Historical data suggest that this cost has increased continuously over the past years. This suggests the need for a more direct means to address the issue. Although it is impossible to completely eliminate corrosion, it is obvious that the best way to address corrosion from an economic stand point will be prevention. An effective prevention technique involves the use and application of corrosion resistant lubricants. More specifically, Corrosion inhibitors added as additives in lubricants help prolong the service life of equipment subject to corrosive service as the useful life of equipment is reduced by corrosion. This on the long run reduces the cost of corrosion.

This research focuses on lubricating grease and proposes a novel grease composition with improved corrosion resistant/protective property.

1.2 Corrosion Protection and Industry Relevance

Corrosion is generally a challenging problem in the industry. Critical equipment components must be protected from corrosion in order to ensure longevity and service reliability. Prior to completion of most industrial designs, the effect of corrosion on the equipment lifespan would need to be considered.

Steel is the most common engineering material, it gives advantages of both mechanical strength and relatively low cost, however it is the most susceptible to corrosion under actions of humidity, acid rain, and salt spray. These are the natural potential hazard associated with oil and gas production and transportation facilities. The piping, pipelines and subsea hardware would gradually become degraded depending upon the fluctuating well conditions. This results in the loss of mechanical properties like strength (compressive, tensile and impact), ductility and toughness. This leads to material loss, thickness reduction, and ultimately, failure. At this point the materials will need to be replaced and production is halted; in addition, the large-scale ecological damage caused by spillage would need to be remediated [3]. Corrosion inhibitors added as additives in lubricating grease provide improved protection against corrosive elements. Having the right grease formulation can help prevent/reduce degradation process and save cost.

1.3 Process of Corrosion

Corrosion being a natural process is the continuous deterioration of a material (metals and polymers) due to its reaction with its environment. Just like water flows towards the lowest level, all processes with energy built into it would natural tend to release energy and go toward a lower energy state [2]. A piece of metal left exposed to moisture will corrode, going back to its lower energy state. The process is even quicker if it is exposed to a corrosive medium, in this case, brine. The Corrosion cycle of steel is shown in Figure 1 below:

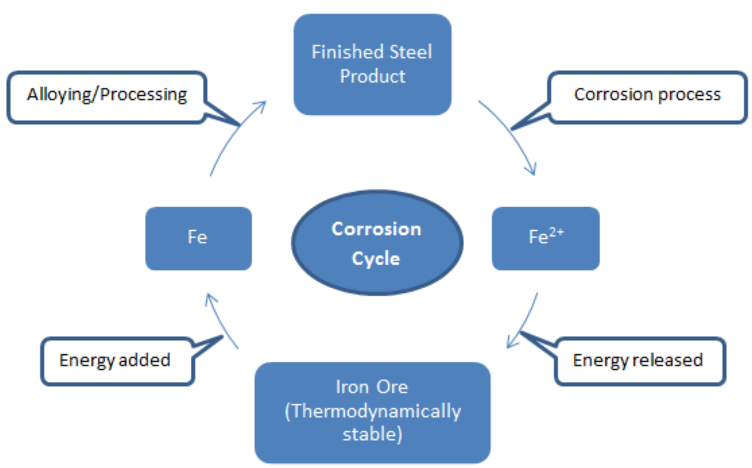

Figure 1. Corrosion Cycle of Steel. [2]

The widely-known electrochemical process that occurs due to oxidation of steel results in the formation of rust and consequently returning steel to its lower energy state. Figure 2 below shows the electrochemical process in the formation of rust.

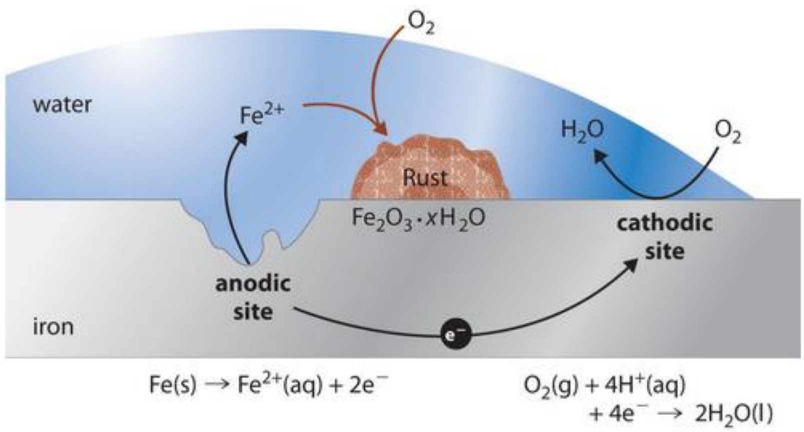

Figure 2. Rust-The Result of Corrosion of Metallic Iron [4].

This electrochemical process is made up of three components: a cathode, an anode and an electrolyte. The material loss occurs at the anode, the medium that permits the transfer of electrons is the electrolyte, the electrons lost at the anode is recovered at the cathode. Hence the cathode completes the electrochemical cell. [5].

According to [6] there are 8 forms of corrosion. The forms of corrosion potentially related to this research include: uniform or general attack, pitting, intergranular corrosion and erosion corrosion. These forms of corrosion are characterized in Table I-1.

Table I-1 Forms of Corrosion [6]

Forms of corrosion	Characteristics
Uniform or General Attack	• Reaction proceeds uniformly. • Metal becomes thinner and eventually fails. • Equipment service life can be accurately estimated
Pitting	• A localized form of corrosion initiated by a break in the protective oxide film • Typically a hole or a cavity • Corrosion proceeds aggressively, hence described as one on the most destructive types of corrosion • It often goes undetected.
Intergranular corrosion	• Localized attack at the grain boundaries. • Mechanical properties are seriously affected.
Erosion corrosion	• Occurs due to the relative motion between the corrosive medium and the surface of the metal. • Material is lost as dissolved ions. • Usually exhibits directional pattern on the metal surface.

1.4 Methods of Corrosion Protection

According to NACE, corrosion control can be achieved with four common methods. They include cathodic protection, materials selection, protective coatings and linings, and corrosion inhibitors. Of these four methods, corrosion inhibitors provide the most efficient, cost effective and proactive approach to combating corrosion and one of the most useful, industry-wide. Corrosion inhibitors are substances that reduce the progression of attack on a material. They extend the service life of equipment, prevent unplanned maintenance, shutdowns, failures, and preserve the aesthetic value of structures [7]. Table I-2 gives a general description of each of the four common methods of corrosion control.

Table I-2 Methods of Corrosion Protection [8]

Corrosion Control	**Features**
Coatings and linings	• Provide a barrier of corrosion-resistant material. • Principal approach for defending against corrosion • Complete coverage is necessary. • Small gaps in coatings can cause extensive damage. • Often used in conjunction with cathodic protection
Cathodic protection	• Electrons are supplied to the metal either by an external source of power or by a galvanic couple • Empirical determination of protective currents. • Commonly used for buried tanks or gas pipelines
Materials selection	• Use of corrosion-resistant materials • Not a cost effective approach for capital intensive projects.
Corrosion inhibitors	• Suppress or Prevent electrochemical reactions. • Protects the base metal by formation of a protective film • One of the most useful approach, industry-wide • Low cost.

1.5 Galling

This form of wear is caused by microscopic transfer of materials between metallic surfaces in sliding contact. When sliding surfaces are pressed together, the initial mating points are the asperities or high points on the surface. Depending on material properties and under conditions of low to moderate surface stress, the high points slide over each other without damage. However under high surface stress, the lubricant film becomes too thin to provide total surface protection, the surfaces will not slide past each other. The high points will then shear and lock together, greatly increasing friction and heat [9]. This consequently leads to cold welding and the material being sheared off the sliding surfaces (See Figure 3), but friction reduction and wear protection is then only provided through the boundary lubrication additives.

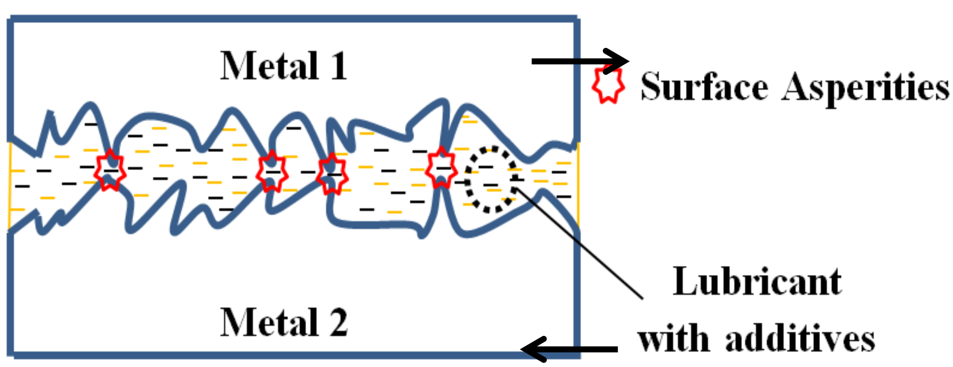

Figure 3. Mating Surface Showing Asperities and Additives.

This form of material loss is often associated with poor lubrication in threaded connections. Specific relevance in oilfield directional drilling, as drill pipe connections will need to be made up under conditions of high surface load and contact stresses. Oilfield thread forms require products with high film strength and specific coefficient of frictional properties. Because thread faces are often subjected to bearing stresses in excess of 50,000 psi, additional downhole connection engagement can result in bearing stresses capable of rupturing the protective "anti-seize" film. This additional engagement can result in wear, galling or complete connection failure [10]. Solid lubricants are used as anti-seize compounds in threaded connections, reducing friction and providing a sealing function for threaded pipe assembly [11]. Solid lubricants are also used in applications of low sliding speed and high contact stress such as for gear lubrication.

1.6 Lubricating Grease

Lubrication, whether with lubricating oil or grease focuses on building an oil film between two mating surfaces that move relative to each other. Compared to oil, grease has the advantage of retention. It can be easily retained between lubricated surfaces and improve the sealing arrangement against moisture and other contaminants. A good grease for a given application must at all times reduce friction and wear; and most importantly protect against rust and corrosion. ASTM defines lubricating grease as: "A solid to semifluid product of dispersion of a thickening agent in liquid lubricant. Other ingredients imparting special properties may be included" [12].

As the definition indicates, three elements (oil, thickener and additives) make up the lubricating grease. The base oil and additives are the major elements in the grease formulation therefore, play a major role in the characterization of the grease. The thickener is the sponge or suspending medium that holds the lubricant [13].

1.7 Composition of Lubricating Grease

As shown in Figure 4 below the usual grease composition is made up of 70 - 95% base oil, 3 - 30% of thickener and 0 - 10% of additives.

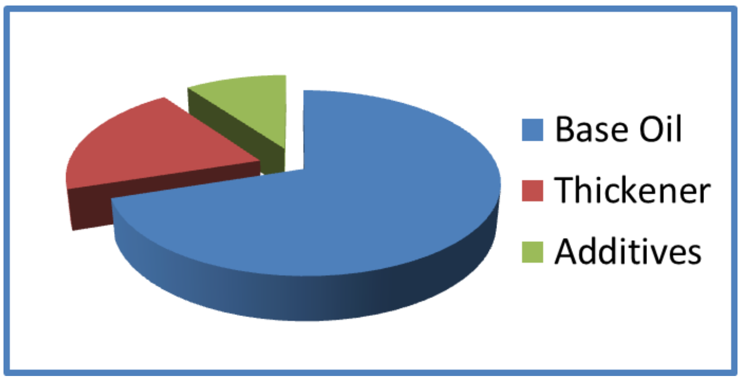

Figure 4. Grease Composition

1.7.1 Base Oil

The largest component of the lubricant, and the part that does the bulk of the work, is the base oil. As depicted in Figure 4, the base oil makes up the largest share of the grease composition. The base oil can be either man-made (synthetic) or nature made (refined petroleum) [14]. Synthetic oils have the advantage of a higher Viscosity index; lower Pour point and it is less volatile. However more expensive, synthetic oils are more desirable than mineral oils.

1.7.2 Thickener

People mostly think grease is primarily thickener but, in actuality, it is mostly oil. Grease contains a thickener like soap fibers pictured in Figure 5, which hold lubricating oil in suspension.

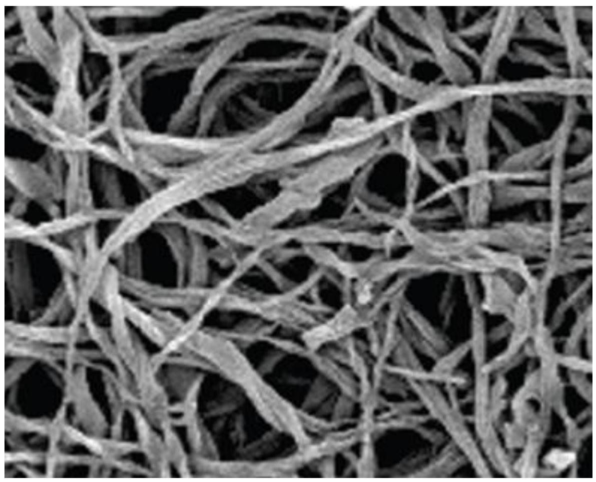

Figure 5. Thickeners in Grease [15].

This is the component in lubricating grease that sets grease apart from fluid lubricants. Thickeners also commonly referred to as viscosity modifiers change the viscosity of lubricants across a range of temperatures. All base oils thin out as the temperature rises. Viscosity modifiers slow down the thinning process [14]. The thickener influences the operating temperature, speed, load and material compatibility of the lubricant. It holds the lubricant in place. Metallic soaps are the primary type of thickener used in current grease. These soaps include lithium, clay, sodium, aluminum polyurea and calcium [13].

1.7.3 Additives

Additives can generally be used to improve desirable features, remove undesired ones and add new attributes to a lubricant. Some of the more important additives used in formulation greases are listed in Table I-3.

Table I-3. Types of Additives and Functions [16]

Additive	Functions
Anticorrosion	Slows deterioration of non-noble metal
Antioxidant	Prolongs life of base oil by increasing the oxidation resistance
Antirust	Slows corrosion of iron alloys
Antiwear	Helps protect loaded metal surfaces by forming a protective film
Color/ultraviolet die	Visual markers for inspection or assembly
Conductive agent	Adds thermal or electrical conductivity
Extreme pressure	Solid burnish into surface under pressure forming a protective layer to prevent seizure and severe damage
Friction modifier	Reduces the coefficient of friction
High-temperature enhancer	Boosts high temperature limit of oil
Tackifier	Increases ability to adhere to moving parts
Viscosity modifiers	Alters oil viscosity

Anticorrosion and Antioxidant additives will be elaborated more upon in this work as they both serve a protective function and hence prolong the service life of equipment subject to corrosive service.

1.7.3.1 Antioxidant Additives

An antioxidant is a molecule that inhibits the oxidation of other molecules. Antioxidant additives retard the degradation of lubricating grease, which in turn prevents oxidation of the ferrous material exposed to a corrosive medium. Oxidation causes of oil thickening which manifests as varnish and sludge formation leading to poor lubrication and corrosive wear [7]. Anti-oxidants are designed to prolong the life of a lubricant by increasing the oxidative resistance of the base oil.

Oxidation occurs in a three-step process: Initiation, Propagation and Termination. If unmitigated, oxidation can lead to the breakdown of the lubricant make-up. A lot more free radicals would be formed during the Propagation step compared to the amount consumed during the termination step as long as the external conditions promote this process. Antioxidants disrupt the degradation process by reacting with free radicals and forming stable species [17]. Antioxidants are additives that protect lubricants from oxidative degradation, allowing it to meet the specified requirements for use in engines and other industrial applications [7].

1.7.3.2 Anticorrosion Additives

A corrosion inhibitor is added as an additive into the grease matrix in relatively small concentrations in order to control the rate or eliminate corrosion [18]. Adding corrosion inhibitors to a lubricant will help slow the deterioration process in non-noble metals. The inhibitors form an inactive film on the metal surface by complexing with metallic ions at the surface. Some corrosion additives work by neutralizing corrosive acids formed from oil and additive degradation byproducts. The inhibitory effect can be quite complex. For example, in organic amines, the additive gets adsorbed on both the anode and cathode and this represses the corrosion process. Some inhibitors are more specific in action and affect either the anodic or cathodic process. Others simply work by forming a protective film on the metal surface [2].

Corrosion inhibitors are classified by the method by which they provide protection. They either are used to treat the fluid medium the metal is in contact with, vaporize and collect on the treated surface, adsorb to the surface, induce passivation, or provide cathodic protection. Also oxygen scavengers are used to remove or isolate the corrosive species in the fluid medium. In an alkaline or near-neutral solution the scavenger may be used to reduce the oxygen content [19].

In this report, the effectiveness of some selected anticorrosion grease additives were analyzed and investigated. The wear and friction performance was also reported.

1.7.3.3 Boundary Lubrication Additives

Lubricant additives such as friction modifiers, EP additives and anti-wear agents are added to lubricants to prevent or reduce the impact of metal-to-metal contact. As the name implies boundary lubrication additives provides a boundary between interacting surfaces thereby reducing wear and friction. When lubricated metallic surfaces are in contact, boundary lubrication additives react with the surface and form a protective surface film which is generally low friction and wear resistant [7].

Having a lubricant with improved frictional performance can help prevent sliding surfaces from galling. Friction modifiers added as additives in lubricating grease minimize the effect of surface contact that occurs during equipment operation by creating a layer of ductile material on the surface thereby reducing the shear strength and become sacrificial [20]. Anti-wear agents work based on a similar mechanism as friction modifiers. They stick to the surface of the metal, and form a protective film which shears under wear conditions. For a light frictional contact, these molecules provide a cushioning effect. In case of a heavy contact, the molecules become insignificant, thereby eliminating the potential benefit of the additive [21]. Extreme pressure additives are the best choice when high surface temperatures are expected. These additives form a low-shear-strength, soap-like film with metal surface reactions and can withstand fairly high temperatures [20].

Since boundary layer additives work by simply improving the frictional performance of the surfaces in contact, the effectiveness of the proposed additives as boundary layer additives are investigated in this research and the frictional performance is reported.

CHAPTER II

MOTIVATION AND OBJECTIVES

As discussed in the previous chapter, material loss in the form of corrosion and wear is money down the drain. Also it could result in catastrophic failures and loss of lives. It is clear that the best way to combat corrosion and wear is by prevention. Nano-sized particles added as additives in lubricating grease help in extending the service life of equipment exposed to corrosive service, thereby promoting smooth industrial operations, and reducing wear losses. This on the long run reduces the cost associated with material losses. There are two objectives in this research:

- To obtain feasibility in a novel method to prevent corrosion and wear.
- To gain understanding in effects of selected additives on corrosion and wear.

In this study, an attempt was made to reduce the rate of corrosion of steel exposed to a corrosive medium. This was done by adding small amounts of CeO_2, Y_2O_3 and Al_2O_3 as anti-corrosion additives to commercial grease. Their effectiveness was individually assessed and reported. The practical significance of this research lies in improving commercial grease lubricants using anticorrosion additives for corrosive wear applications. The approaches are as follows:

1) Evaluate the effectiveness of CeO_2, Y_2O_3 and Al_2O_3 as anti-corrosion additives

2) Evaluate wear and friction performance of samples of the novel grease.

Detailed experimental procedures will be discussed in Chapter III.

CHAPTER III

EXPERIMENTAL PROCEDURES

This chapter discusses the materials and experimental approaches used for this research. Nano-sized CeO_2, Y_2O_3 and Al_2O_3 were used as additives in lubricating grease. The experimental approach majorly involves using two different equipment: the Galling equipment and the salt spray chamber. The galling equipment was used for the friction test while the salt spray chamber was used for the corrosion test. Figure 6 shows a flowchart summarizing the activities, resources and results obtained in this research. Other devices used include: the optical microscope for surface examination and the measuring scale. Experimental details and procedures are explicitly detailed.

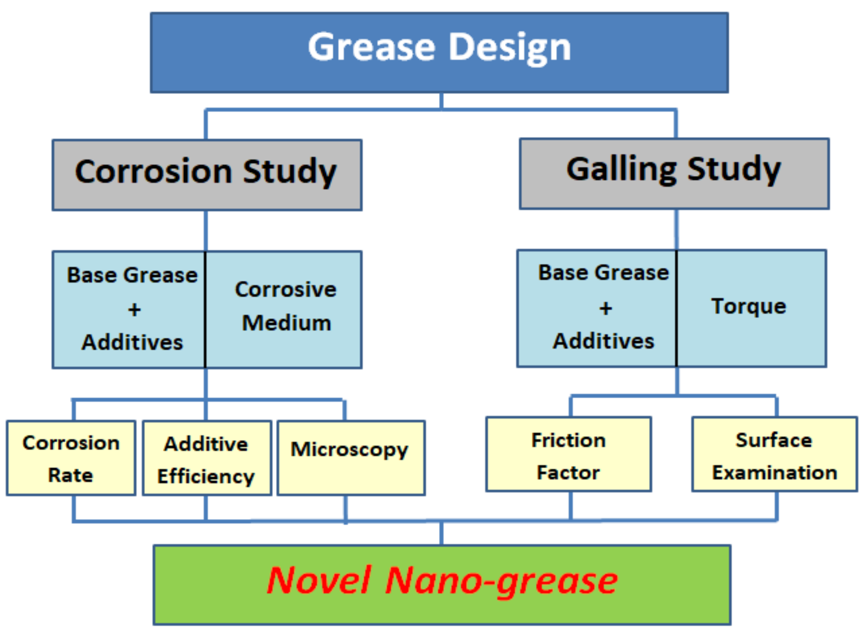

Figure 6. Experimental Flow Chart

3.1 Nanoparticle as Additives

In this chapter, all three compounds used as additives are briefly discussed and justification is provided for their possible use as additives in lubricating grease. The strategy of selection and their properties will be provided.

3.1.1 Cerium Oxide (CeO_2)

3.1.1.1 Properties

Cerium Oxide (CeO_2), or also known as cerium dioxide, is formed from a binary compound of oxygen bonding with the sparse earth metal cerium. This compound is a subtle yellow color in powder form and possesses a cube-like crystal structure [22]. Cerium oxide is most commonly found in its powder form, but can be transformed into other forms such as tablets, granules, and pieces. Cerium oxide (CeO_2) is the most stable oxide of cerium [23]. Although cerium oxide is insoluble in water, it is soluble in strong mineral acids [22]. The compound also possesses a unique property allowing it to reversibly convert to a nonstoichiometric oxide. Under a wide range of conditions, ceria maintains an oxygen vacancy. This is the most stable and dominant defect in ceria. Neutral oxygen vacancies may be generated by a reversible transition from Ce^{3+} to Ce^{4+} [23]. Under oxidizing conditions, nanoceria is able to store oxygen (Ce^{4+}), however under reducing conditions, oxygen is released (oxygen vacancies are created, hence formation of Ce^{3+}) [24]. This property of CeO_2 makes it suitable to be used as an antioxidant additive in grease.

Table III-1. Properties of Cerium Oxide [22].

Chemical Formula	CeO_2
Appearance	White or pale yellow solid
Crystallography	Face Centered Cubic (FCC)
Molar mass	172.114 g/mol
Density	7.215 g/cm^3
Melting point	2670 K
Boiling point	3770 K
Mohs Hardness @ 20 °C	6
Solubility in H_2O	Insoluble
Magnetic susceptibility	+2.60 *10^{-6} cm^3/mol

3.1.1.2 Applications

The unique chemical stability and physical properties of Cerium Oxide (CeO_2) makes them suitable for quite a number of applications, and in recent years there have been increased studies into its application and uses. CeO_2 can be found in most glass cleaning agents, especially glass cleaners. It is used as a polishing agent and used to decolorize glass. Cerium Oxide can also be used as much more than a cleaning agent such as an abrasive, additive in paint, and an absorbent [22]. Due to its unique characteristic to reversibly convert into a nonstoichiometric oxide, CeO_2 is commonly used in automotive operations [25]. This compound can expel oxygen of a combustion engine in the exhaust steam. With the help of other catalysts, cerium can transform the harmful emissions from carbon monoxide (CO) into carbon dioxide. Cerium can be used as an aid catalyst in the conversion of diesel fuel into carbon dioxide (CO_2) and hydrogen gas (H_2); it has been shown that increase in the oxygen defect concentration of this compound will also increase its catalytic ability and activities [25].

3.1.2 Yttrium Oxide (Y_2O_3)

3.1.2.1 Properties

Yttrium oxide also called Yttria is one of the most important and widely used compounds of the element Yttrium. It is used in making YVO_4 europium, and Y_2O_3 europium phosphors to give the red color in color television tubes [26].

A research done by [27] suggests that Y_2O_3 nanoparticles are excellent antioxidants, in other words, Yttria nanoparticles are free radical scavengers due to their non-stoichiometric crystal defects. Free radical scavengers either prevent formation of reactive (oxidative) species, or remove them before causing any damage [28].

The key properties of Yttrium Oxide are as shown:

Table III-2. Properties of Y_2O_3 [29]

Mechanical	
Crystal Structure	Cubic
Density	5.033 g/cm^3
Melting Point	2410 ^oC
Young's Modulus	25.3 x 106 psi (zero porosity)
Thermal	
Thermal conductivity (50–200°C)	0.12-0.08 W/cm·^oC.
Thermal expansion	8.1 x 10-6/°C
Specific heat (25–1000°C)	0.13
Linear Expansion	9.3 x 10^{-6} in. per in. per ^oC to 1400 ^oC

3.1.2.2 Applications

Yttrium oxide is used as sintering additives for the formation of SiC ceramics [30] used in high endurance applications such as in car clutches and brakes and ceramic plates in bulletproof vests. Yttrium oxide nanoparticles doped with Europium is a well-known phosphor material is used in making plasma and flat panel displays, fluorescent lamps and photoelectric sensors.

In high temperature applications such as titanium alloy casting, yttrium oxide is used as an additive in coating crucibles, tuyeres and nozzles for improved resistance to molten metals prepared by rapid solidification [29].

3.1.3 Aluminum Oxide (Al_2O_3)

3.1.3.1 Properties

Aluminum Oxide (Al_2O_3), a geometrically octahedral chemical compound consisting of aluminum and oxygen, can be found in nature in a myriad of minerals. In its most common form, which is called corundum or α-aluminum oxide, it is an odorless white crystalline that is insoluble in absolute alcohol [31]. Figure 7 shows the arrangement of atoms in a cell of Al_2O_3. It has a trigonal crystal structure represented by the hexagonal cell [32]. This form of aluminum oxide is created at high temperatures. The chemical compound, Al_2O_3, has a melting point of 2345 K and a boiling point of 3250 K. Aluminum oxide exhibit excellent dielectric characteristics. Considering aluminum oxide is regarded to be a ceramic material, it has a comparably high thermal conductivity rate of 30 $Wm^{-1}K^{-1}$ [31].

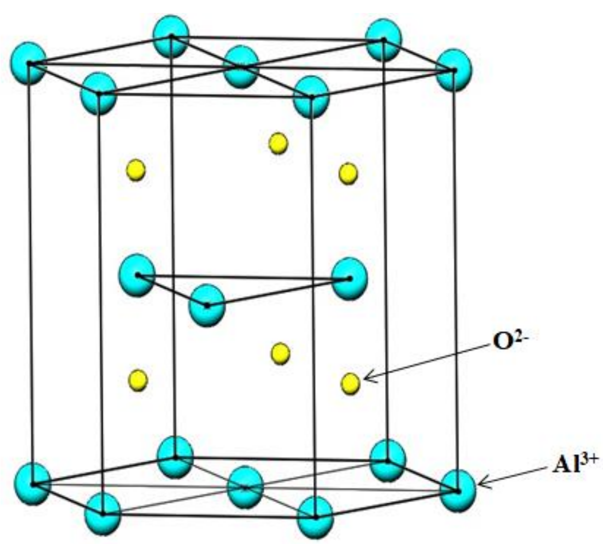

Figure 7. Crystal Structure of Al_2O_3 [33]

With their large crystal lattice structure and several covalent bonds, these compounds are also insoluble in water. Aluminum Oxide has a molar mass of approximately 101.948 g/mol with a density of 3.986 g/cm^3 [31]. Due to the compact and impenetrable nature of the compound, Al_2O_3 can be used as an abrasive material and an element in cutting hard substances like tools. In most cases, metallic aluminum will respond to the mix of oxygen in the atmosphere but with a layer of aluminum oxide on the surface [34]. Metallic aluminum is highly responsive to oxygen and the effects of weather so the layer of aluminum oxide is particularly necessary to protect the surface of the material from corroding.

Unlike the other oxides Al_2O_3 proves its specialty by being the only oxide that is amphoteric. Aluminum oxide is classified as amphoteric because it displays both acidic and basic properties. In its most common form known as corundum, the chemical compound becomes unreactive. Due to the compound's large crystal lattice structure mentioned above, Al_2O_3 does not react with water. Although aluminum oxide is unlike the other oxides, it does react with acids in the same way sodium or magnesium oxides do. This is due to the oxide ions that the compound contains.

Depending on the level of purity, values posted on Table III-3 represent properties of Al_2O_3 between 94% and 99.5% purity [34].

Table III-3. Mechanical, Thermal and Electrical Properties of Al_2O_3 [34].

Mechanical	Units of Measure	SI/Metric[1]
Density	gm/cc	3.69-3.89
Porosity	%	0
Flexural Strength	MPa	330 - 379
Elastic Modulus	GPa	300 - 375
Shear Modulus	GPa	124 - 152
Bulk Modulus	GPa	165 - 228
Poisson's Ratio	—	0.21 - 0.22
Compressive Strength	MPa	2100 - 2600
Hardness	Kg/mm^2	1175 - 1440
Fracture Toughness K_{IC}	$MPa•m^{1/2}$	3.5 – 4.0
Maximum Use Temperature (no load)	°C	1700 - 1750
Thermal		
Thermal Conductivity	W/m°K	18 - 35
Coefficient of Thermal Expansion	10^{-6}/°C	8.1 - 8.4
Specific Heat	J/Kg•°K	880
Electrical		
Dielectric Strength	ac-kv/mm	16.7 - 16.9
Dielectric Constant	@ 1 MHz	9.1 - 9.8
Loss Tangent	@ 1 kHz	—
Volume Resistivity	ohm•cm	$>10^{14}$

3.1.3.2 Uses/Occurrences

With its durable characteristics and variety of form, aluminum oxide can be used in a number of ways. If we were to create a list of all the products formed from Al_2O_3, the list would be extremely extensive. This compound is highly used in engineering and in many industries. As stated above, aluminum oxide is a very hard and durable material,

[1] From 94% to 99.5% Al_2O_3

making it an excellent abrasive material. This compound is popular in the ceramic industry as an insulating substance. Al_2O_3 is also used in manufacturing, specifically for refractories [35]. Since refractories must be able to withstand pressure and heat, aluminum oxide works as a good component to use in the making of refractory machines due to its relatively high boiling point. Aluminum oxide is commonly used as a protective layer for different materials [35]. This is because this substance does not react with the oxygen in the atmosphere, making it an ideal compound to be used in the prevention of wear, tear, and rust.

3.2 Grease Preparation

The Calcium Fluoride (CaF_2) bolt lube standard formulation, which is a NLGI grade 1 lithium grease, was used as the base grease or reference compound. The weight percentage composition is as provided in Table III-4 below. The NLGI number provides a means of expressing the relative hardness of lubricating grease. This classification is as provided by the National Lubricating Grease Institute (NLGI).

Table III-4. CaF_2 Bolt Lube Standard Formulation [36]

Component	Percent by Weight
Lithium Grease NLGI 1	55.0 ± 1.0
Calcium Fluoride Superfine	35.0 ± 1.0
Calcium sulfate	8.0 ± 0.50
Vanlube 73	2.0 ± 0.50

Base grease mixed with the proposed additives in 1 wt% and 3 wt% compositions was prepared. The mixing was done by hand until a uniform dispersion of the additive particles in the grease matrix was achieved. Prior experimental runs invalidated the use of V_2O_5 as an anticorrosion additive hence it was discontinued. CeO_2, Y_2O_3 and Al_2O_3 additives showed significant improvement and were further analyzed.

3.3 Sample Preparation

For the corrosion experiment, 8 steel coupons were used per composition (1 wt% and 3 wt%) of grease sample, making a total of 56 samples. Initial surface preparation was done to prepare the steel coupons getting rid of existing surface rust and other surface deposits. Abrasive paper was used for the surface preparation process after which the surface was cleaned with ethanol and the initial weights measured and recorded.

Figure 8 shows the steel coupons. The back and sides of the steel coupons were coated and protected with water resistant epoxy leaving the top surface exposed. A thin film of the grease samples was then applied on the exposed surface. For a controlled corrosion process, the steel coupons have to be protected as such.

Figure 8. Steel Coupons

Water resistant epoxy efficiently protected the coupons from moisture, improving the overall reliability of the results. Spray paint was used in prior experimental runs but blisters were observed after the exposure period which affected the accuracy of the result.

3.4 Salt Spray Test

This is a standard corrosion test method used to carry out accelerated corrosion test to check corrosion resistance of materials and surface coatings. ASTM B117 provides the standard testing requirement/procedure for operating the salt spray equipment. The apparatus required for the salt spray (fog) test consists of a fog chamber, a brine reserve, a supply of compressed air, at least one atomizer, specimen supports, provision for the chamber temperature regulation and control. Figure 9 and Figure 10 respectively show the labeled exterior and interior views of the salt spray equipment

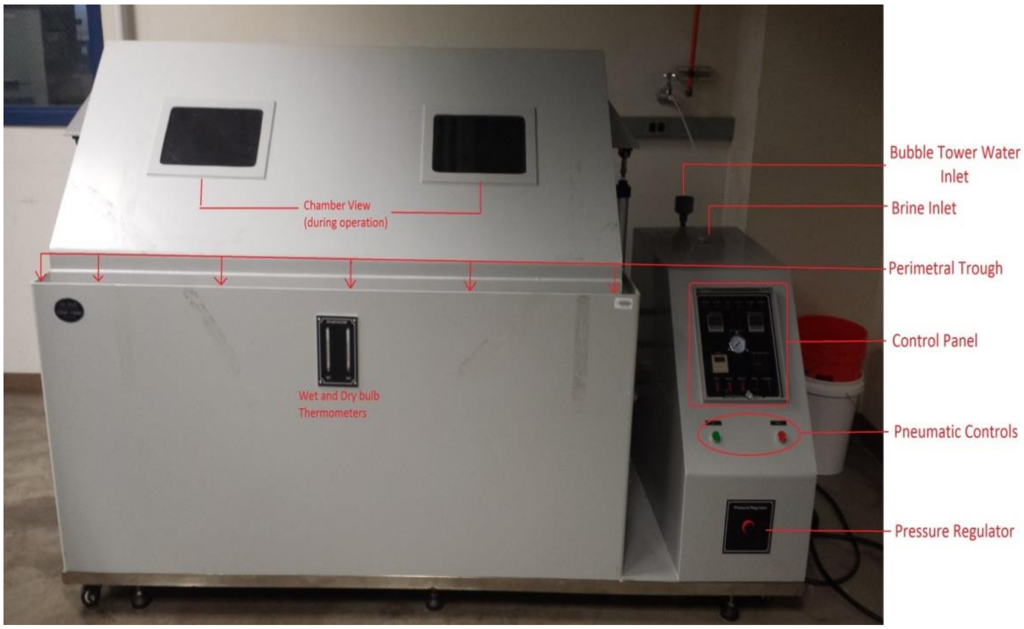

Figure 9. Exterior of the Salt Spray Equipment

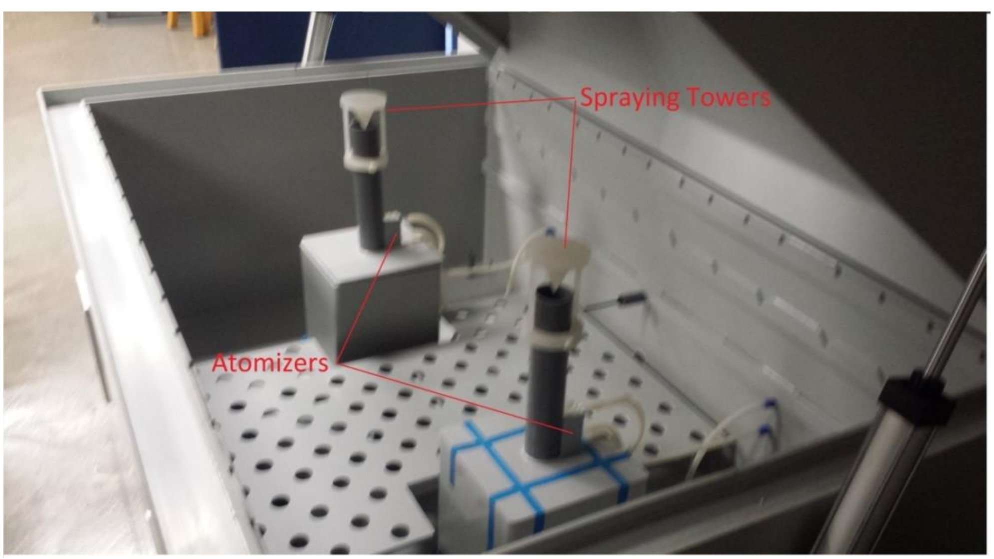

Figure 10. Interior of the Salt Spray Equipment

The operating conditions in the salt spray chamber was set and maintained at a temperature of 35^{o}C. The brine solution was made to 5% weight concentration (pH between 6.5 and 7.2) and the exposure time was 336 hours (2weeks).

The steel samples were suspended on the specimen support as shown in Figure 11 below. This is in accordance with Clause 7 in ASTM B117 that is, parallel to the principal flow direction of the fog.

Figure 11. Position of Specimens during Exposure

3.5 Standard API RP 7A1 Tests

This recommended practice provides recommendations for testing the frictional performance of thread compound for rotary shouldered connections. This test was carried out in order to analyze the effectiveness of the grease samples as threaded compounds. As previously mentioned, seven grease samples were used. The thread compounds are applied between the surfaces of two cylindrical test specimens (static and dynamic specimen) and reversible torque cycles (make up and break out) are applied. Data acquisition is done concurrently, recording the torque, rotation, load and so on.

3.5.1 Test Equipment

Figure 12 shows a schematic diagram of the apparatus. The test apparatus consist of 6 main sections: The Motor/gearbox provides the rotation and the required torque to the test specimen with speed set at 3 RPM. The second section is the Torque transducer which resists the applied rotation and sends back signal which is proportional to the applied torque. The third section is the Rotation transducer which gives feedback on the degree of rotation of the specimen. The control panel provides manual control functions while the Computer/DAQ provides automated control functions. The hex socket and the load cell make up the Cartridge assembly.

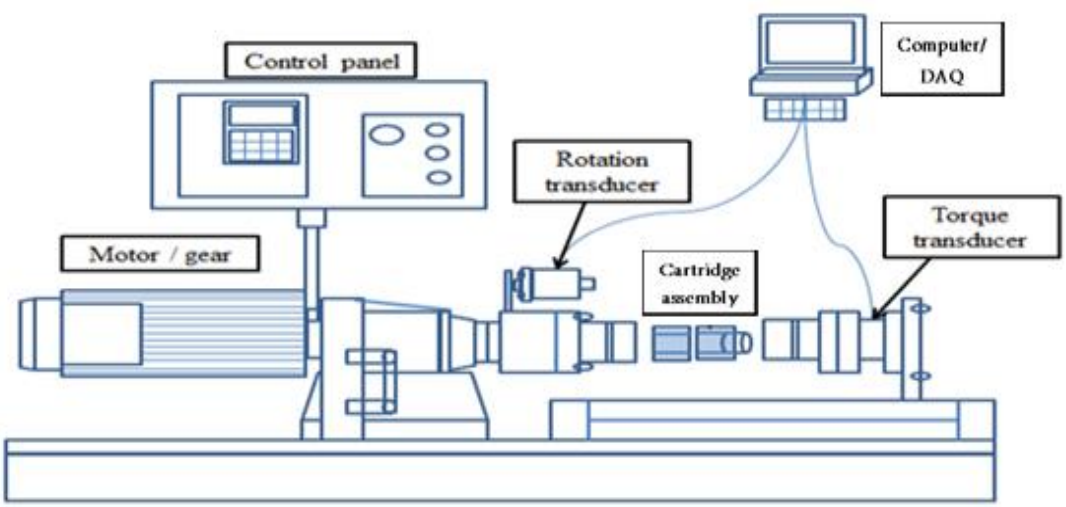

Figure 12. API RP 7A1 Test Apparatus [36]

3.5.2 Galling Test Specimen

The static and dynamic specimens are made of Inconel A-718. This material is used because of its excellent mechanical properties and susceptibility to galling. It combines corrosion resistance and high strength. This alloy is used in spacecrafts, rocket motors, nuclear reactors, gas turbines, pumps and tooling [37].

Table III-5 and Table III-6 respectively show the chemical composition and Physical properties of Inconel A-718.

Table III-5. Limiting Percentage Composition of Inconel A-718 [38]

Element	%	Element	%	Element	%
Ni + Co	50.0 – 55.0	Ti	0.65 – 1.15	Si	0.35 max.
Cr	17.0 -21.0	Al	0.20 – 0.80	P	0.015 max.
Fe	Remainder	Co	1.0 max.	S	0.015 max.
Nb + Ta	4.75 - 5.50	C	0.08 max.	B	0.006 max.
Mo	2.80 – 3.30	Mn	0.35 max.	Cu	0.30 max.

Table III-6. Physical Constants and Thermal Properties of Inconel A-718 [39]

Density	8.19 g/cm^3
Melting Range	1260 – 1336 ^{o}C
Specific Heat	435 J/kg ^{o}C
Permeability at 200 Oersted	1.0011
Coefficient of Expansion	13.0 µm/m ^{o}C between 21 – 93^{o}C
Thermal Conductivity	11.4 W/m ^{o}C

3.5.3 Test Procedure

Before proceeding with the test cycles, initial equipment calibrations will be done. The readings on the torque cell and load cell must be zeroed out. The upper and lower torque limit is set to 200 ft-lbs and 300 ft-lbs respectively on the configuration menu. Data is recorded within these torque limits.

A thin film of grease is applied on the dynamic and static specimen after which is it made-up hand-tight and placed in the test machine. It should be noted that the initial or hand-tight torque should not exceed 14 N-m (10 ft-lb). The make up cycle is started and continues until the load reaches the set load value which is typically 55,000lbs. The Break out process starts as soon as this set value is reached. As the name suggests, this process simply involves unloading the specimen by rotating in the opposite direction. Generated data is collected and stored on the computer as the make up and break up cycles run.

Between 5 and 10 cycles make up a test run for either the test compound or the reference compound. A complete test consists of three runs, i.e. a calibration run using the reference compound; a run with the test compound; and a repeat run using the reference compound. A total of 24 cycles (8 cycles each) were conducted for each grease compound in order to obtain an optimized test condition and data with adequate repeatability and confidence.

After each cycle the specimen is cleaned with a degreaser and visually inspected for any signs of galling on the mating surfaces.

The friction factor of the grease samples may be obtained after data analysis is done. The grease sample has a higher frictional performance relative to the reference compound if the friction factor is greater than 1.

The flow chart in Figure 13 below shows the testing procedure for a complete cycle. These steps would need to be repeated 24 times (3 runs) for a complete test of a grease sample.

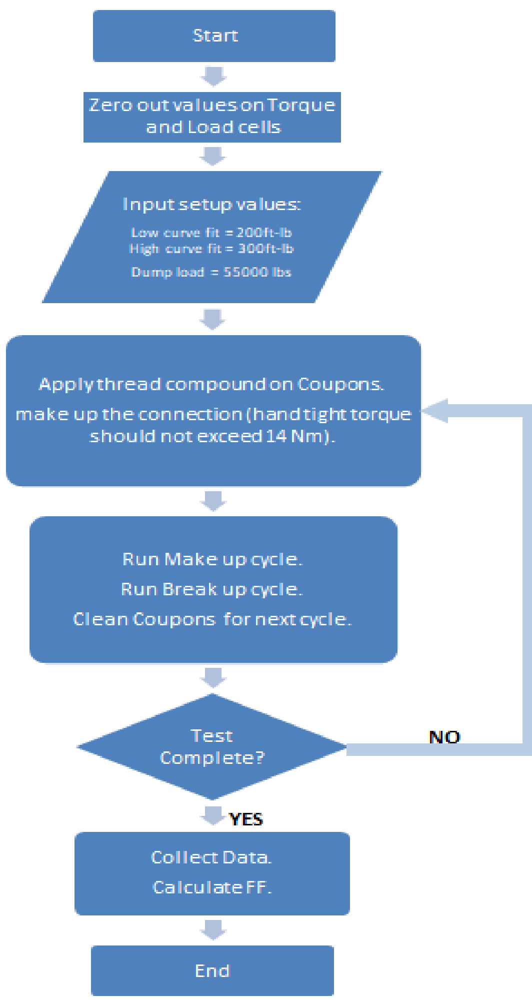

Figure 13. Testing Procedure for the Galling Test.

CHAPTER IV

EFFECTS OF OXIDE PARTICLE ADDITIVES ON CORROSION

This chapter focuses on the study of effects of CeO_2, Y_2O_3 and Al_2O_3 additives on corrosion. Corrosion results obtained using the salt spray chamber were presented. Analysis on removal rate correlating to the addition of CeO_2, Y_2O_3 and Al_2O_3 particles was conducted. Compared with base grease, it was observed that all three additives significantly reduced the corrosion rate. The best result was obtained when Al_2O_3 additive was used.

4.1 Effects of Particle Additive on Corrosion Rate

The corrosion rate of steel samples was evaluated using a salt spray chamber. Experimental conditions and procedures have been discussed in Chapter III, subheadings 3.2 - 3.4. The effects of additives are evaluated.

After 336 hours (2 weeks) of exposure, the steel coupons were removed from the salt spray equipment and cleaned. Corrosive losses under the six protective grease samples were measured. By comparing the corrosion rates with that of base grease, the effectiveness of various grease additives were evaluated. Figure 14 illustrates the results of the corrosion test. As indicated in the previous chapter, the experiment was conducted using eight steel coupons per grease sample, this was done for result consistency and to collect a wide range of data points.

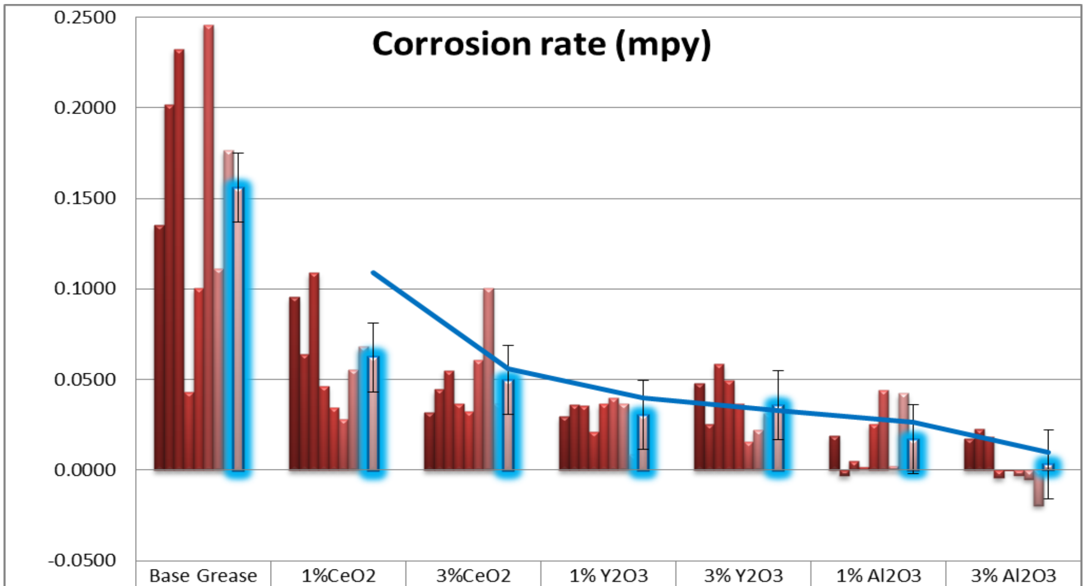

	Base Grease	1%CeO2	3%CeO2	1% Y2O3	3% Y2O3	1% Al2O3	3% Al2O3
1	0.1351	0.0953	0.0319	0.0293	0.0478	0.0188	0.0174
2	0.2018	0.0637	0.0443	0.0362	0.0255	-0.0032	0.0226
3	0.2324	0.1088	0.0548	0.0354	0.0585	0.0051	0.0182
4	0.0428	0.0460	0.0366	0.0211	0.0493	0.0017	-0.0044
5	0.1004	0.0343	0.0324	0.0364	0.0363	0.0251	-0.0006
6	0.2458	0.0277	0.0608	0.0399	0.0154	0.0441	-0.0029
7	0.1113	0.0555	0.1003	0.0366	0.0220	0.0022	-0.0052
8	0.1767	0.0680	0.0367	0.0086	0.0313	0.0422	-0.0196
Average	0.1558	0.0624	0.0497	0.0304	0.0358	0.0170	0.0032
Std.Dev.	0.0705	0.0282	0.0230	0.0106	0.0150	0.0187	0.0147

Figure 14. Corrosion rate in Mills per Year

Based on average values, the plot of the corrosion rate is shown in Figure 15 below.

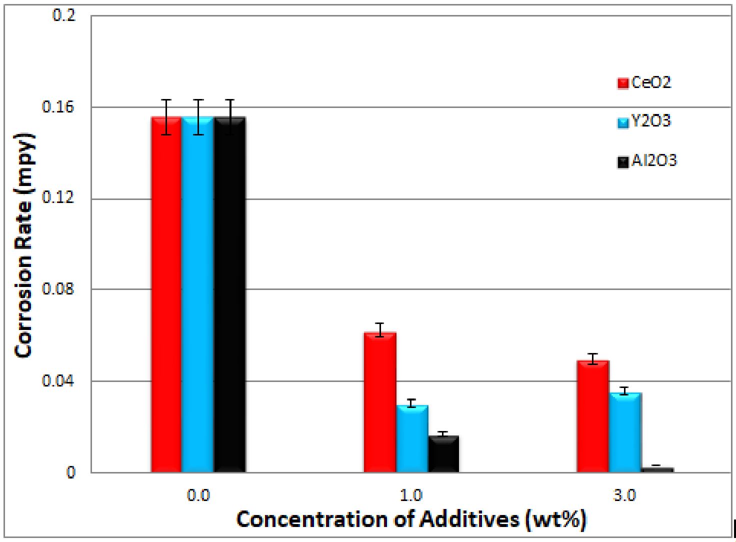

Figure 15. Average corrosion rates.

The weight loss was determined and the corrosion rate evaluated using the following equation:

$$corrosion\ rate\ (mm/year) = 534\ \frac{W}{D \times A \times T}$$

W: Weight loss (mg)

A: Area of steel specimen (in^2)

T: Exposure time (h)

D: Density of steel (7.87 g/cm^3).

It was observed that the corrosion rate was the highest with only base grease applied. In order of decreasing magnitude we have:

$$Base\ grease \gg CeO_2 > Y_2O_3 > Al_2O_3$$

It may also be observed that the higher additive composition (3% wt.) provides better corrosion protection than the lower additive composition (1% wt.). Interesting results were obtained with Al_2O_3 additives. However being the lowest, the negative corrosion rates indicate a weight gain after the exposure period. Although the phenomenon responsible for this weight gain is not fully understood on finer levels, It may be attributable to surface adherence and Al_2O_3 forming a protective oxide layer on the surface of the steel coupons which prevents attack on the surface and consequently lead to weight gain.

4.1.1 Additive Efficiency on Corrosion Prevention

The Additive efficiency can be calculated by the following equation:

$$E_f = \frac{R_o - R_a}{R_o} \times 100$$

where, E_f is additive efficiency (percentage), R_a is corrosion rate with additive and R_o is corrosion rate without additive [40].

Based on average values, Table IV-1 presents data for the corrosion rate and the Inhibitor efficiency.

Table IV-1. Additive Efficiency and Corrosion Rate

Grease Sample	Corrosion Rate (mpy)	Additive Efficiency (%)
Base grease	0.156	--
Base grease + 1% CeO_2 Additive	0.062	59.9
Base grease + 3% CeO_2 Additive	0.050	68.1
Base grease + 1% Y_2O_3 Additive	0.030	80.5
Base grease + 3% Y_2O_3 Additive	0.036	77.0
Base grease + 1% Al_2O_3 Additive	0.017	89.01
Base grease + 3% Al_2O_3 Additive	0.003	98.0

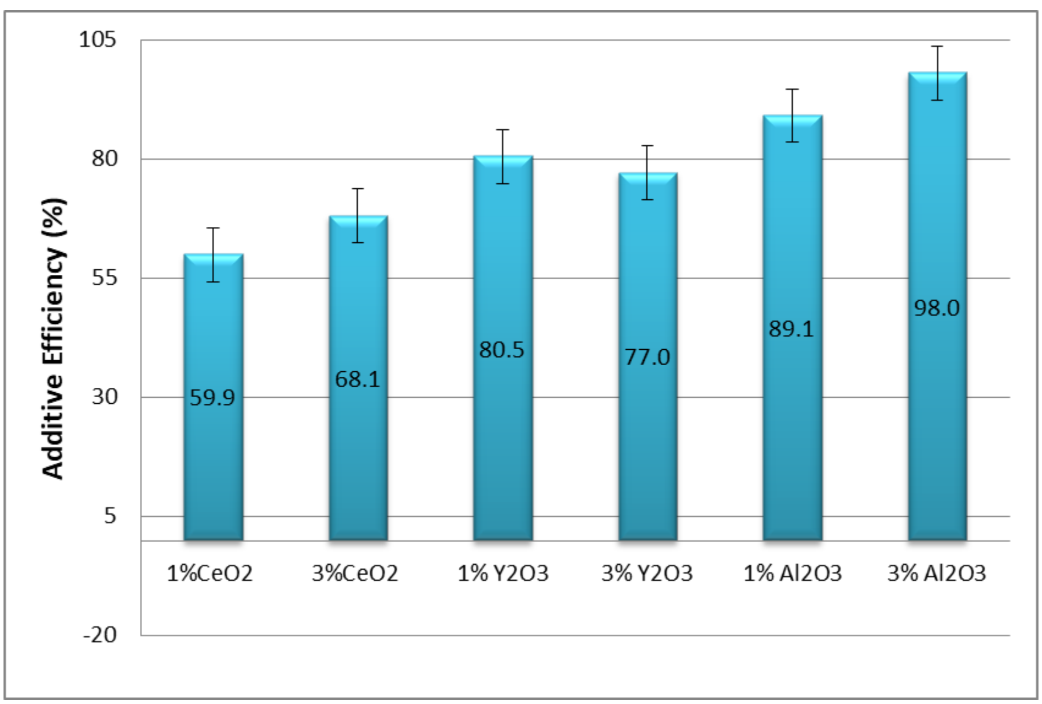

Figure 16. Additive Efficiency

Figure 16 presents a visual representation of the Additive efficiency. From the plot it can be deduced that CeO_2 being the least efficient additive provides an increased efficiency in excess of 50% when only 1% weight composition is used. Also Al_2O_3 at 3% weight composition was the most effective with efficiency at approximately 98%. An interesting observation with the results for Y_2O_3. The grease with 1% Y_2O_3 is slightly more efficient than the 3% Y_2O_3 grease. This would imply that relatively little Y_2O_3 will typically be required as additives in grease.

4.1.2 Corrosion Mode

After data analysis was completed the surface of the corroded steel samples were observed with the optical microscope to determine the nature and form of corrosion.

Figure 17 through Figure 20 are surface microscopic images for a coupon with 1 wt. % Y_2O_3 grease applied. This is a typical example as the forms of corrosion observed are the same as with other applied grease samples.

Figure 17 shows the coupon before the test and Figure 18 is the image after.

Some localized ‘pits’ (detail A) and ‘Erosion corrosion’ (detail B) may be observed in Figure 18. Figure 19 is the magnified imagine of detail A and Figure 20 is a magnified image of detail B, showing features of the eroded surface. It can be observed that the ridges on the surface become more distinct and the grain boundary becomes clearly defined.

‘Uniform corrosion’, ‘Erosion corrosion’, and ‘Pitting’ corrosion were observed on the surface.

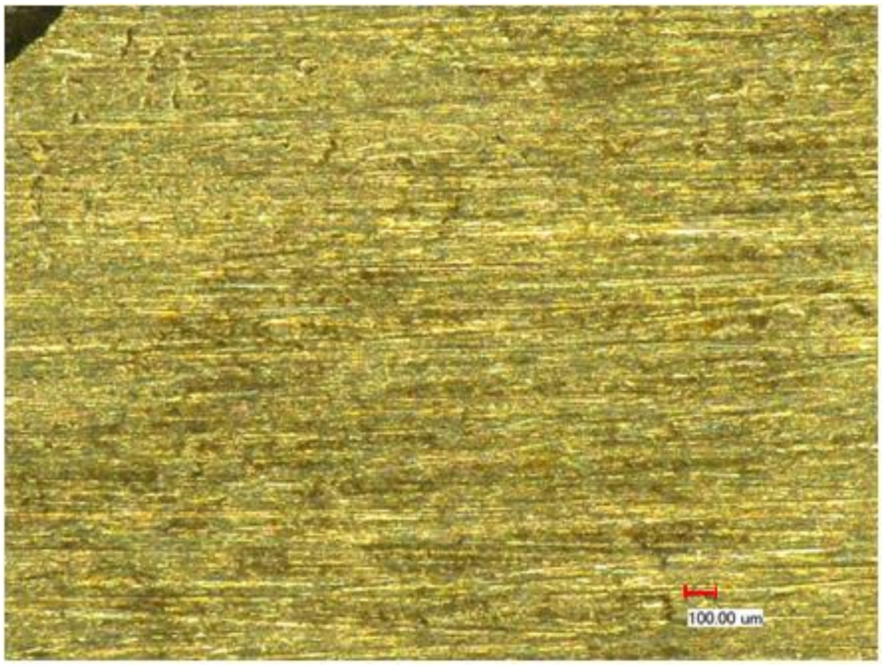

Figure 17. Coupon before Corrosion – Magnification: 100x

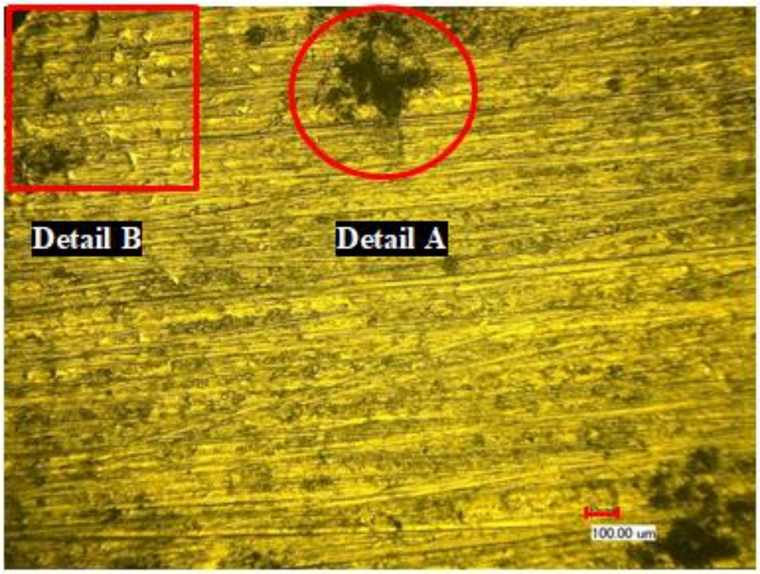

Figure 18. Coupon after Corrosion – Magnification: 100x

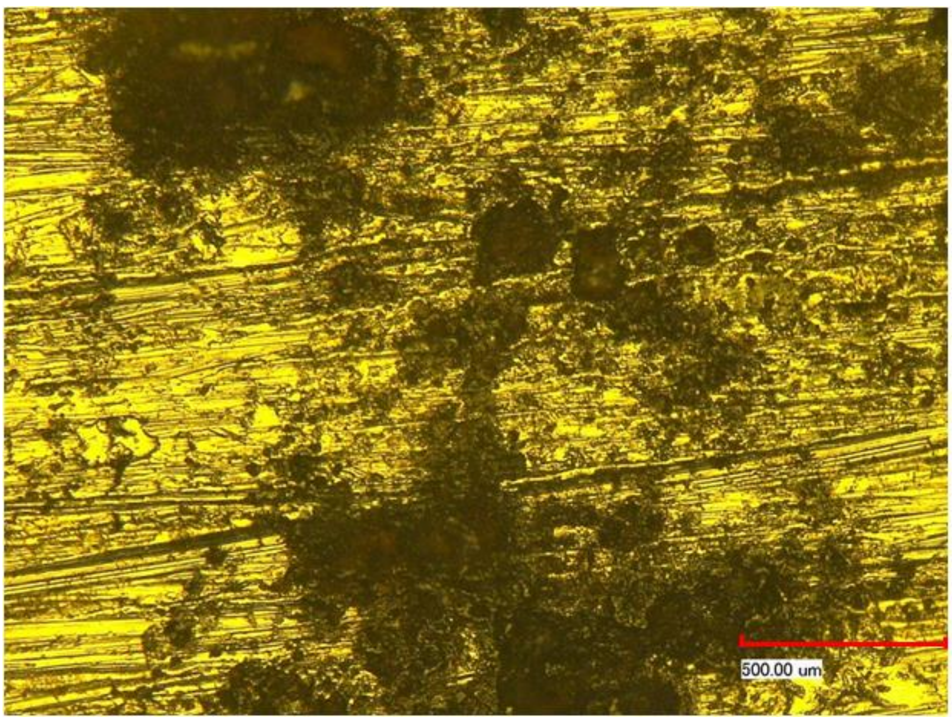

Figure 19. 'Detail A' – Magnification: 500x

Zooming into detail B:

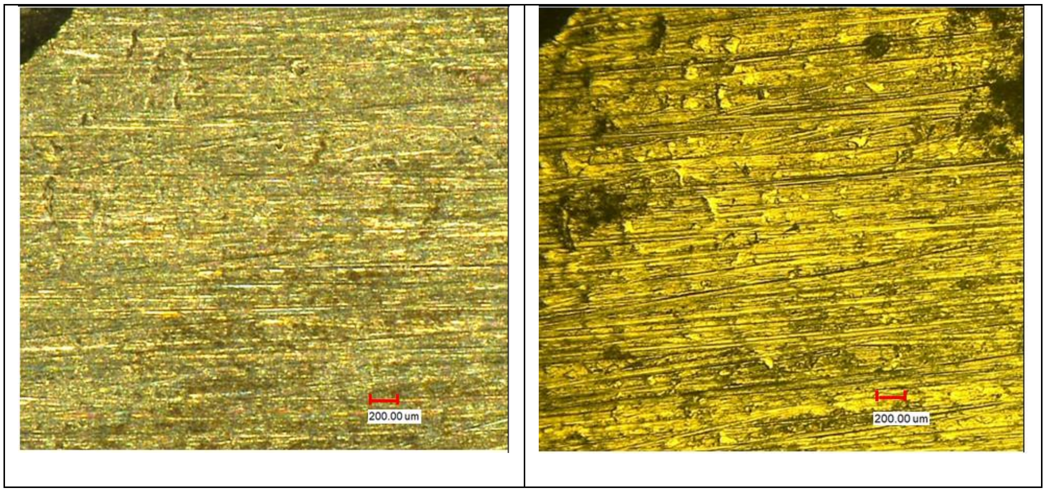

Figure 20. 'Detail B' – Magnification: 200x (before and after respectively)

Figure 21 and Figure 22 are surface microscopic images for a coupon with 1 wt. % CeO_2 grease applied.

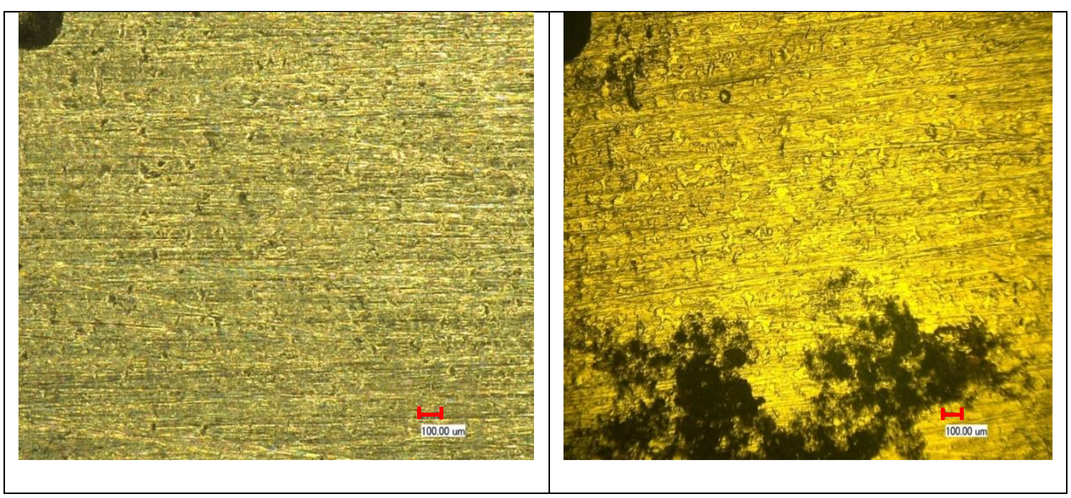

Figure 21. Magnification: 100x (before and after respectively)

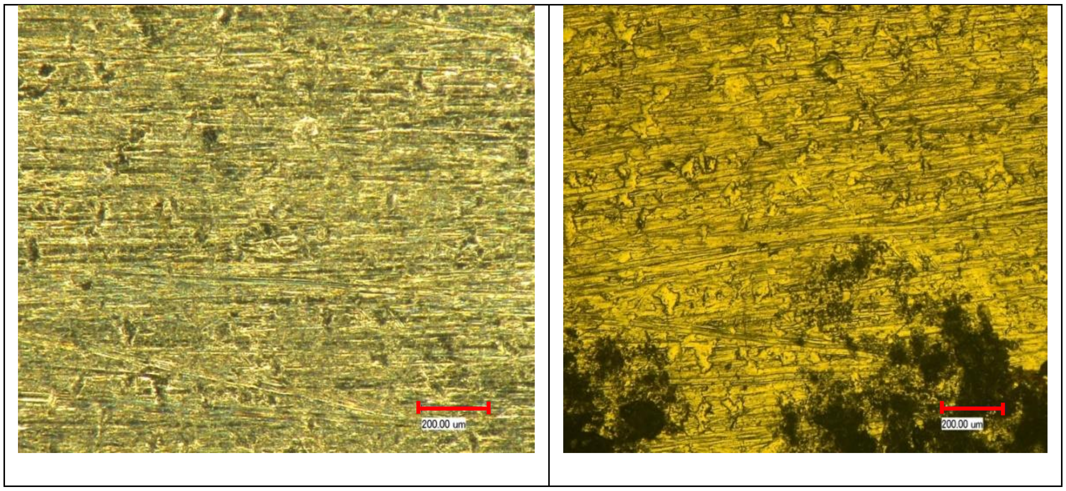

Figure 22. Magnification: 200x (before and after respectively)

Figure 23 and Figure 24 are surface microscopic images for a coupon with 1 wt. % Al_2O_3 grease applied.

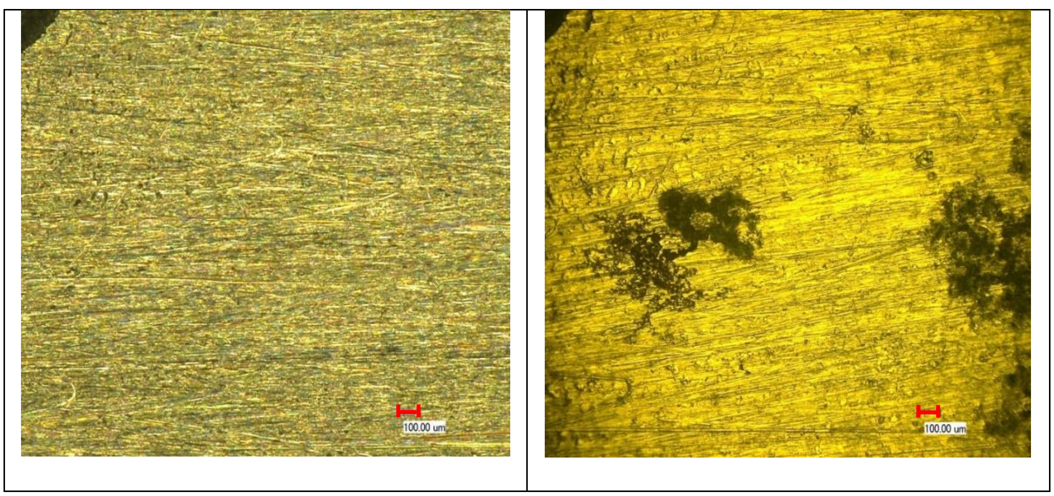

Figure 23. Magnification: 100x (before and after respectively)

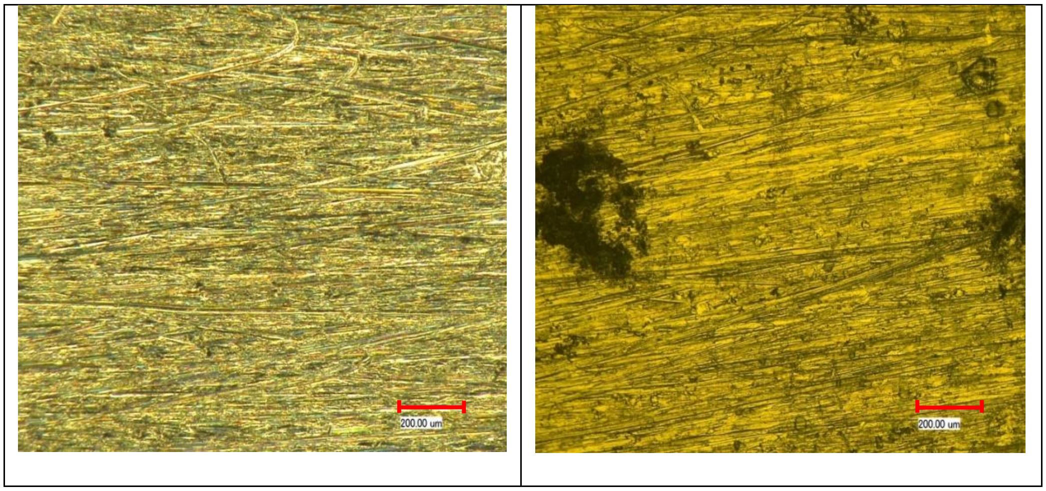

Figure 24. Magnification: 200x (before and after respectively)

4.1.3 Mechanism of Additive Action in Corrosion Protection

Lubricant additives may be either organic or inorganic. Corrosion inhibitors provide a protecting layer on metal surfaces [41]. Based on the type of additives, the mechanism of additive action at reducing corrosion is by either anodic or cathodic action and/or by adsorption. In general, inorganic corrosion additives work by anodic or cathodic actions while organic corrosion additives have both actions, that is, reaction type (anodic and cathodic) and by film adsorption [42]. Inorganic additives used in this research play a distinct role in reducing corrosion. The anodic and cathodic inhibitory effect is brought about by the reaction of the additives with metallic ions ejected from the surface. This produces and deposits insoluble hydroxides on the surface forming an insoluble film restricting the diffusion of reducible species. Insufficient amounts of inhibitor could affect the formation of the protective film, leaving parts of the metal surface exposed to localized corrosion.

In this research it is suggested that insoluble metallic hydroxides such as $Al(OH)_3$, $Ce(OH)_4$, $Y(OH)_3$ and hydroxides of Iron are formed which further deters the degradation process. Table IV-2 shows the solubility of the metallic hydroxides. The low solubility values confirm the proposed mechanism. Based on the amount of additives, it is not likely a full film of hydroxides was formed. However, it was enough to show potential effects in corrosion protection. Future research will be carried out to characterize the nature of surface reaction products.

Table IV-2. Solubility of Metallic Hydroxides [43], [44].

Compound	Formula	Solubility (K_{sp} (25 °C))
Aluminum Hydroxide	$Al(OH)_3$	3.00×10^{-34}
Cerium Hydroxide	$Ce(OH)_4$	1.60×10^{-22}
Yttrium Hydroxide	$Y(OH)_3$	1.00×10^{-22}
Iron(II) hydroxide	$Fe(OH)_2$	4.87×10^{-17}
Iron(III) hydroxide	$Fe(OH)_3$	2.79×10^{-39}

CHAPTER V

EFFECTS OF OXIDE PARTICLE ADDITIVES ON GALLING

This chapter focuses on the study of effects of CeO_2, Y_2O_3 and Al_2O_3 additives on galling. The galling resistance and frictional properties of the grease compounds are tested. Friction data obtained using the galling test equipment were presented. Analysis of the wear and friction factor correlating to the addition of CeO_2, Y_2O_3 and Al_2O_3 particles was conducted. Compared with the reference compound, the best result was obtained when 1% Al_2O_3 and 1% Y_2O_3 additives were used. They exhibited good friction-reduction and anti-galling properties.

5.1 Galling and Friction Tests

Galling tests were conducted using the API standard testing equipment as described in Chapter III, Subheading 3.5. Samples were tested with make-up (350ft-lbs) and break out torque cycles. After each cycle, the specimen is visually inspected for any signs of wear or galling. A galled specimen means the grease sample failed to provide adequate surface lubrication; the grease compound is rejected and the test is complete. The cylindrical specimen will then need to be sent to a machine shop and re-faced to a proper surface roughness. In the series of tests conducted, no signs of galling was observed indicating the effectiveness of all three additives. Figure 25 shows the specimen after the test.

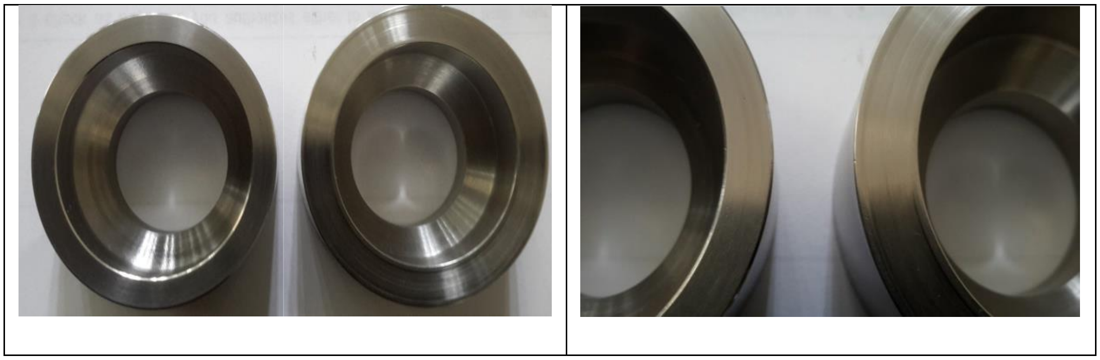

Figure 25. Visual Examination of Specimen Surface.

The tribological performance of the grease samples was evaluated in terms of friction factor. The make-up torque for threaded connections can be approximated with knowledge of the friction factor of a thread compound. [45]. With the same degree of rotation, a high friction factor indicates that a higher torque is needed to make up the specimen. In other words, a higher FF will allow you to apply more torque (which is good), while still maintaining the rated stress level of the material. Lower torque values are not as good since they do not provide as good a seal. A thread compound with FF >1 is better than one with FF <1.

The friction factor can be calculated as shown below:

$$\mathrm{FF} = \frac{2 \cdot S_2}{S_1 + S_3}$$

S_1 is the average slope of the first calibration run (8 cycles) using the reference compound.

S_2 is the average slope of the 8 cycles using the test thread compound.

S_3 is the average slope of the second calibration run (8 cycles) using the reference compound.

As mentioned in the previous chapter, the effectiveness of six grease samples were tested against base grease and for the API RP 7A1 test, a complete test consists of three runs, i.e. a calibration run using the reference compound; a run with the test compound; and a repeat run using the reference compound. Table V-1 through Table V-6 presents results for the grease samples.

The Make Up (M/U) torque is the maximum torque reached during the make up process and in a similar manner, the Break Out (B/O) torque is the maximum torque reached during the break out process, i.e. when loosened in the opposite direction of rotation. Figure 26 shows a typical plot for the torque and force against rotation.

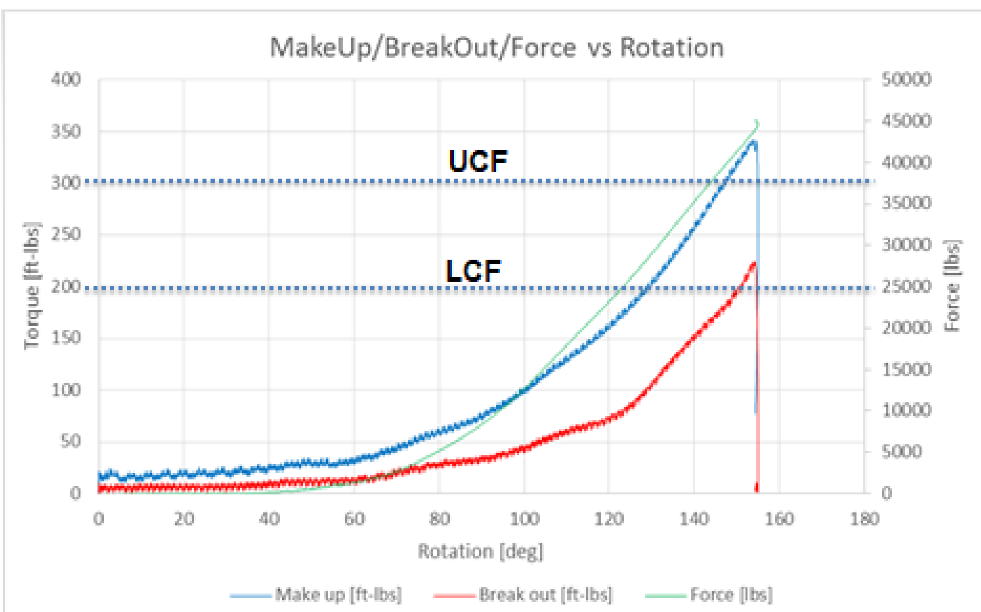

Figure 26. Data Plot for the Reference compound

The Upper (≈ 300 ft-lbs) and Lower (≈ 200 ft-lbs) Curve Fit represent a range of torque limits within which the slope may be calculated. At least 20 pairs of data points (curve fit points) are needed. The slope represents the result of the test and its calculated by the least squares fit of a straight line to the torque versus rotation data over the upper and lower curve fit ranges [36]. Max. Load and Angle respectively represent the maximum values of load and rotation reached during the test and this has a direct correlation with the grease performance.

Table V-1. Friction Test Result for Thread compound with 1% CeO_2 Additive

Run No.	Thread Compound	M/U Torque (ft-lbs)	B/O Torque (ft-lbs)	B/O to M/U Ratio	Upper Torque Curve Fit (ft-lbs)	Lower Torque Curve Fit (ft-lbs)	Points Curve Fit	Slope of Line (ft-lbs/deg)	Max Load [lbs]	Max Angle [degrees]
1	Reference	342.0	224.5	65.62	303.5	200.0	139	5.61	45079	155
2	Reference	343.0	223.7	65.23	301.0	202.3	148	4.99	46758	207
3	Reference	352.2	222.4	63.16	301.0	201.9	150	4.91	49317	203
4	Reference	353.7	219.6	62.10	302.2	200.2	155	5.03	51468	187
5	Reference	349.8	220.1	62.92	302.1	203.4	149	5.33	49952	186
6	Reference	347.9	219.6	63.14	303.6	200.8	162	5.38	48616	179
7	Reference	350.0	225.1	64.30	300.6	201.1	153	5.00	49186	182
8	Reference	345.4	220.1	63.73	302.0	204.3	156	4.79	50311	166
Average		348.0	221.9	63.78	302.0	201.8	152	$\boxed{5.13}$	48836	183
Std.Dev.		4.2	2.3	1.20	1.1	1.5	7	0.28	2042	17

Run No.	Thread Compound	M/U Torque (ft-lbs)	B/O Torque (ft-lbs)	B/O to M/U Ratio	Upper Torque Curve Fit (ft-lbs)	Lower Torque Curve Fit (ft-lbs)	Points Curve Fit	Slope of Line (ft-lbs/deg)	Max Load [lbs]	Max Angle [degrees]
1	1% CeO_2	345.6	220.6	63.84	301.6	200.5	152	5.06	47426	183
2	1% CeO_2	346.0	215.1	62.15	300.8	201.7	157	5.11	47410	205
3	1% CeO_2	343.7	219.3	63.79	300.2	202.2	154	5.16	48127	174
4	1% CeO_2	344.5	216.9	62.94	300.2	200.4	141	5.64	48290	185
5	1% CeO_2	345.3	220.6	63.89	300.2	200.8	156	5.17	52185	171
6	1% CeO_2	343.6	207.6	60.42	302.4	202.1	149	5.23	49594	190
7	1% CeO_2	345.3	209.2	60.58	300.2	201.1	147	5.17	50376	200
8	1% CeO_2	346.7	219.5	63.31	301.4	200.2	146	5.43	49415	209
Average		345.1	216.1	62.62	300.9	201.1	150	$\boxed{5.25}$	49103	190
Std.Dev.		1.1	5.1	1.43	0.8	0.8	5	0.19	1637	14

Run No.	Thread Compound	M/U Torque (ft-lbs)	B/O Torque (ft-lbs)	B/O to M/U Ratio	Upper Torque Curve Fit (ft-lbs)	Lower Torque Curve Fit (ft-lbs)	Points Curve Fit	Slope of Line (ft-lbs/deg)	Max Load [lbs]	Max Angle [degrees]
1	Reference	354.3	227.0	64.07	302.3	201.3	149	5.58	48241	198
2	Reference	346.4	219.6	63.39	303.9	200.8	161	5.27	49056	192
3	Reference	352.1	219.9	62.47	304.6	200.6	156	5.30	50637	189
4	Reference	351.5	222.7	63.36	301.0	200.8	146	5.44	48078	188
5	Reference	337.7	213.0	63.08	302.1	201.8	162	5.11	46628	180
6	Reference	343.1	214.1	62.39	300.9	200.0	154	5.54	49415	206
7	Reference	353.3	220.9	62.52	300.5	200.8	150	5.62	52707	204
8	Reference	347.5	216.5	62.31	300.5	203.1	148	5.50	48860	205
Average		348.2	219.2	62.95	302.0	201.2	153	$\boxed{5.42}$	49203	195
Std.Dev.		5.7	4.6	0.63	1.6	0.9	6	0.18	1826	9

The first set of results shown in Table V-1 above represents the test data and results for the thread compound with 1% CeO_2 additive. The average slope of the first 8 cycles (calibration run) with the reference compound is 5.13; the average slope of the next 8

cycles (with thread compound) is 5.25; and the average slope of the last 8 cycles using the reference compound again is 5.42.

The friction factor is then calculated to be 0.995 which indicates that the friction factor is slightly lower than that of the reference compound. In other words, 1% CeO_2 additive reduces the frictional properties of the reference compound by 0.5%.

Table V-2. Friction Test Result for Thread compound with 3% CeO_2 Additive

Run No.	Thread Compound	M/U Torque (ft-lbs)	B/O Torque (ft-lbs)	B/O to M/U Ratio	Upper Torque Curve Fit (ft-lbs)	Lower Torque Curve Fit (ft-lbs)	Points Curve Fit	Slope of Line (ft-lbs/deg)	Max Load [lbs]	Max Angle [degrees]
1	Reference	354.3	227.0	64.07	302.3	201.3	149	5.58	48241	198
2	Reference	346.4	219.6	63.39	303.9	200.8	161	5.27	49056	192
3	Reference	352.1	219.9	62.47	304.6	200.6	156	5.30	50637	189
4	Reference	351.5	222.7	63.36	301.0	200.8	146	5.44	48078	188
5	Reference	337.7	213.0	63.08	302.1	201.8	162	5.11	46628	180
6	Reference	343.1	214.1	62.39	300.9	200.0	154	5.54	49415	206
7	Reference	353.3	220.9	62.52	300.5	200.8	150	5.62	52707	204
8	Reference	347.5	216.5	62.31	300.5	203.1	148	5.50	48860	205
Average		348.2	219.2	62.95	302.0	201.2	153	$\boxed{5.42}$	49203	195
Std.Dev.		5.7	4.6	0.63	1.6	0.9	6	0.18	1826	9

Run No.	Thread Compound	M/U Torque (ft-lbs)	B/O Torque (ft-lbs)	B/O to M/U Ratio	Upper Torque Curve Fit (ft-lbs)	Lower Torque Curve Fit (ft-lbs)	Points Curve Fit	Slope of Line (ft-lbs/deg)	Max Load [lbs]	Max Angle [degrees]
1	3% CeO_2	349.2	221.5	63.44	304.0	201.1	151	5.55	49463	199
2	3% CeO_2	351.2	220.1	62.66	302.6	202.9	143	5.39	49496	193
3	3% CeO_2	347.4	214.2	61.64	304.9	201.0	149	5.69	46986	190
4	3% CeO_2	349.0	217.0	62.18	302.2	200.4	151	5.69	47948	180
5	3% CeO_2	343.1	214.4	62.49	301.6	202.5	153	5.62	48681	198
6	3% CeO_2	351.8	220.4	62.64	302.0	201.7	151	5.62	49643	195
7	3% CeO_2	345.2	212.0	61.42	300.0	200.3	154	5.39	50670	198
8	3% CeO_2	352.3	222.2	63.09	303.7	201.3	176	4.86	47051	155
Average		348.7	217.7	62.45	302.6	201.4	154	$\boxed{5.48}$	48742	189
Std.Dev.		3.3	3.9	0.68	1.5	0.9	10	0.28	1320	15

Run No.	Thread Compound	M/U Torque (ft-lbs)	B/O Torque (ft-lbs)	B/O to M/U Ratio	Upper Torque Curve Fit (ft-lbs)	Lower Torque Curve Fit (ft-lbs)	Points Curve Fit	Slope of Line (ft-lbs/deg)	Max Load [lbs]	Max Angle [degrees]
1	Reference	339.4	217.0	63.94	300.2	200.4	153	5.71	50490	195
2	Reference	345.0	215.9	62.60	304.2	201.5	165	5.31	47508	161
3	Reference	351.2	221.3	63.02	301.0	201.7	159	5.27	47720	190
4	Reference	346.6	218.2	62.95	302.9	200.1	162	5.30	49056	189
5	Reference	346.4	221.5	63.95	300.1	201.9	164	5.23	50995	202
6	Reference	343.1	213.0	62.09	304.9	201.1	154	5.88	48681	213
7	Reference	351.6	219.0	62.28	300.8	202.3	148	5.89	51778	198
8	Reference	348.7	220.0	63.10	301.7	200.4	154	5.65	49121	206
Average		346.5	218.2	62.99	302.0	201.2	157	$\boxed{5.53}$	49419	194
Std.Dev.		4.1	2.9	0.69	1.8	0.8	6	0.28	1535	16

The first set of results shown in Table V-2 above represents the test data and results for the thread compound with 3% CeO_2 additive. The average slope of the first 8 cycles (calibration run) with the reference compound is 5.42; the average slope of the next 8

cycles (with thread compound) is 5.48; and the average slope of the last 8 cycles using the reference compound again is 5.53.

The friction factor is then calculated to be 1.00 which indicates that the friction factor is approximately same as the reference compound. In other words, 3% CeO_2 additive has little effect on the frictional properties of the reference compound (0.02% increase).

It may be said, however not conclusively, that the friction performance of the thread compound with CeO_2 Additive increases as the additive composition increases.

Table V-3. Friction Test Result for Thread compound with 1% Y_2O_3 Additive

Run No.	Thread Compound	M/U Torque (ft-lbs)	B/O Torque (ft-lbs)	B/O to M/U Ratio	Upper Torque Curve Fit (ft-lbs)	Lower Torque Curve Fit (ft-lbs)	Points Curve Fit	Slope of Line (ft-lbs/deg)	Max Load [lbs]	Max Angle [degrees]
1	Reference	339.4	217.0	63.94	300.2	200.4	153	5.71	50490	195
2	Reference	345.0	215.9	62.60	304.2	201.5	165	5.31	47508	161
3	Reference	351.2	221.3	63.02	301.0	201.7	159	5.27	47720	190
4	Reference	346.6	218.2	62.95	302.9	200.1	162	5.30	49056	189
5	Reference	346.4	221.5	63.95	300.1	201.9	164	5.23	50995	202
6	Reference	343.1	213.0	62.09	304.9	201.1	154	5.88	48681	213
7	Reference	351.6	219.0	62.28	300.8	202.3	148	5.89	51778	198
8	Reference	348.7	220.0	63.10	301.7	200.4	154	5.65	49121	206
Average		346.5	218.2	62.99	302.0	201.2	157	5.53	49419	194
Std.Dev.		4.1	2.9	0.69	1.8	0.8	6	0.28	1535	16

Run No.	Thread Compound	M/U Torque (ft-lbs)	B/O Torque (ft-lbs)	B/O to M/U Ratio	Upper Torque Curve Fit (ft-lbs)	Lower Torque Curve Fit (ft-lbs)	Points Curve Fit	Slope of Line (ft-lbs/deg)	Max Load [lbs]	Max Angle [degrees]
1	1% Y_2O_3	343.1	213.4	62.19	300.2	202.0	147	5.79	48583	194
2	1% Y_2O_3	348.5	212.1	60.86	301.3	200.8	144	6.03	49089	184
3	1% Y_2O_3	340.6	218.1	64.04	304.3	203.1	162	5.55	48828	172
4	1% Y_2O_3	352.1	222.4	63.17	300.4	200.4	161	5.55	48909	171
5	1% Y_2O_3	344.8	217.1	62.97	303.1	202.1	153	5.76	47850	174
6	1% Y_2O_3	345.5	218.8	63.32	303.8	202.7	156	5.62	48274	186
7	1% Y_2O_3	341.8	221.0	64.68	300.4	201.3	163	5.31	48975	156
8	1% Y_2O_3	343.9	221.5	64.41	300.6	202.3	174	5.09	50083	173
Average		345.0	218.1	63.21	301.8	201.8	158	5.59	48824	176
Std.Dev.		3.7	3.7	1.25	1.7	0.9	10	0.29	654	12

Run No.	Thread Compound	M/U Torque (ft-lbs)	B/O Torque (ft-lbs)	B/O to M/U Ratio	Upper Torque Curve Fit (ft-lbs)	Lower Torque Curve Fit (ft-lbs)	Points Curve Fit	Slope of Line (ft-lbs/deg)	Max Load [lbs]	Max Angle [degrees]
1	Reference	344.2	220.9	64.20	303.0	204.1	163	5.33	49708	206
2	Reference	343.1	211.6	61.66	302.1	202.4	156	5.60	46823	183
3	Reference	349.0	217.7	62.37	302.4	201.7	160	5.48	49447	189
4	Reference	340.8	212.2	62.28	300.5	200.5	148	5.79	49366	195
5	Reference	347.5	220.1	63.34	302.3	200.3	171	5.07	50458	184
6	Reference	347.4	226.0	65.05	301.8	200.1	182	4.70	48453	177
7	Reference	347.1	221.5	63.81	304.9	200.0	176	5.21	49154	215
8	Reference	342.5	211.3	61.69	300.8	203.5	162	5.49	50213	178
Average		345.2	217.7	63.05	302.2	201.6	165	5.33	49203	191
Std.Dev.		2.9	5.4	1.24	1.4	1.6	11	0.34	1144	14

The first set of results shown in Table V-3 above represents the test data and results for the thread compound with 1% Y_2O_3 additive. The average slope of the first 8 cycles (calibration run) with the reference compound is 5.53; the average slope of the next 8

cycles (with thread compound) is 5.59; and the average slope of the last 8 cycles using the reference compound again is 5.33.

The friction factor is then calculated to be 1.029 which indicates that the friction factor is higher than that of the reference compound. In other words, 1% Y_2O_3 additive increases the frictional properties of the reference compound by 2.9%.

Table V-4. Friction Test Result for Thread compound with 3% Y_2O_3 Additive

Run No.	Thread Compound	M/U Torque (ft-lbs)	B/O Torque (ft-lbs)	B/O to M/U Ratio	Upper Torque Curve Fit (ft-lbs)	Lower Torque Curve Fit (ft-lbs)	Points Curve Fit	Slope of Line (ft-lbs/deg)	Max Load [lbs]	Max Angle [degrees]
1	Reference	344.2	220.9	64.20	303.0	204.1	163	5.33	49708	206
2	Reference	343.1	211.6	61.66	302.1	202.4	156	5.60	46823	183
3	Reference	349.0	217.7	62.37	302.4	201.7	160	5.48	49447	189
4	Reference	340.8	212.2	62.28	300.5	200.5	148	5.79	49366	195
5	Reference	347.5	220.1	63.34	302.3	200.3	171	5.07	50458	184
6	Reference	347.4	226.0	65.05	301.8	200.1	182	4.70	48453	177
7	Reference	347.1	221.5	63.81	304.9	200.0	176	5.21	49154	215
8	Reference	342.5	211.3	61.69	300.8	203.5	162	5.49	50213	178
Average		345.2	217.7	63.05	302.2	201.6	165	$\boxed{5.33}$	49203	191
Std.Dev.		2.9	5.4	1.24	1.4	1.6	11	0.34	1144	14

Run No.	Thread Compound	M/U Torque (ft-lbs)	B/O Torque (ft-lbs)	B/O to M/U Ratio	Upper Torque Curve Fit (ft-lbs)	Lower Torque Curve Fit (ft-lbs)	Points Curve Fit	Slope of Line (ft-lbs/deg)	Max Load [lbs]	Max Angle [degrees]
1	3% Y_2O_3	349.4	223.9	64.09	304.2	201.8	171	5.11	49920	175
2	3% Y_2O_3	346.0	220.9	63.84	301.9	200.0	170	5.25	51077	214
3	3% Y_2O_3	343.9	215.4	62.64	300.2	201.2	181	4.49	48078	191
4	3% Y_2O_3	344.7	217.1	62.98	302.4	201.6	177	4.78	48958	206
5	3% Y_2O_3	347.9	218.3	62.77	301.5	200.2	184	4.65	49920	204
6	3% Y_2O_3	342.5	219.3	64.01	302.2	200.5	170	5.29	50507	160
7	3% Y_2O_3	344.7	217.4	63.07	301.7	200.5	159	5.60	47003	173
8	3% Y_2O_3	348.6	213.5	61.24	301.6	202.8	151	5.47	49952	176
Average		346.0	218.2	63.08	302.0	201.1	170	$\boxed{5.08}$	49427	187
Std.Dev.		2.4	3.2	0.94	1.1	1.0	11	0.40	1340	19

Run No.	Thread Compound	M/U Torque (ft-lbs)	B/O Torque (ft-lbs)	B/O to M/U Ratio	Upper Torque Curve Fit (ft-lbs)	Lower Torque Curve Fit (ft-lbs)	Points Curve Fit	Slope of Line (ft-lbs/deg)	Max Load [lbs]	Max Angle [degrees]
1	Reference	350.8	222.1	63.31	303.2	200.3	157	5.31	49692	190
2	Reference	343.8	218.2	63.45	300.9	200.2	200	4.36	47622	199
3	Reference	343.1	212.7	61.99	301.8	200.4	183	4.87	48828	193
4	Reference	344.3	217.9	63.28	300.2	202.3	172	5.11	51305	181
5	Reference	343.5	215.5	62.73	300.0	201.4	190	4.53	51077	197
6	Reference	348.8	225.4	64.62	300.1	200.4	189	4.27	48926	204
7	Reference	344.0	215.3	62.58	300.8	201.1	181	4.58	47948	207
8	Reference	345.8	215.6	62.35	302.5	201.0	180	5.00	48209	179
Average		345.5	217.8	63.04	301.2	200.9	182	$\boxed{4.75}$	49201	194
Std.Dev.		2.8	4.1	0.82	1.2	0.7	13	0.37	1386	10

The first set of results shown in Table V-4 above represents the test data and results for the thread compound with 3% Y_2O_3 additive. The average slope of the first 8 cycles (calibration run) with the reference compound is 5.33; the average slope of the next 8

cycles (with thread compound) is 5.08; and the average slope of the last 8 cycles using the reference compound again is 4.75.

The friction factor is then calculated to be 1.007 which indicates that the friction factor is higher than that of the reference compound. In other words, 3% Y_2O_3 additive increases the frictional properties of the reference compound by 0.7%.

It may be said, however not conclusively, that the friction performance of the thread compound with Y_2O_3 Additive decreases as the additive composition increases.

Table V-5. Friction Test Result for Thread compound with 1% Al_2O_3 Additive

Run No.	Thread Compound	M/U Torque (ft-lbs)	B/O Torque (ft-lbs)	B/O to M/U Ratio	Upper Torque Curve Fit (ft-lbs)	Lower Torque Curve Fit (ft-lbs)	Points Curve Fit	Slope of Line (ft-lbs/deg)	Max Load [lbs]	Max Angle [degrees]
1	Reference	350.8	222.1	63.31	303.2	200.3	157	5.31	49692	190
2	Reference	343.8	218.2	63.45	300.9	200.2	200	4.36	47622	199
3	Reference	343.1	212.7	61.99	301.8	200.4	183	4.87	48828	193
4	Reference	344.3	217.9	63.28	300.2	202.3	172	5.11	51305	181
5	Reference	343.5	215.5	62.73	300.0	201.4	190	4.53	51077	197
6	Reference	348.8	225.4	64.62	300.1	200.4	189	4.27	48926	204
7	Reference	344.0	215.3	62.58	300.8	201.1	181	4.58	47948	207
8	Reference	345.8	215.6	62.35	302.5	201	180	5	48209	179
Average		345.5	217.8	63.04	301.2	200.9	182	$\boxed{4.75}$	49201	194
Std.Dev.		2.8	4.1	0.82	1.2	0.7	13	0.37	1386	10

Run No.	Thread Compound	M/U Torque (ft-lbs)	B/O Torque (ft-lbs)	B/O to M/U Ratio	Upper Torque Curve Fit (ft-lbs)	Lower Torque Curve Fit (ft-lbs)	Points Curve Fit	Slope of Line (ft-lbs/deg)	Max Load [lbs]	Max Angle [degrees]
1	1% Al_2O_3	345.6	221.8	64.18	300.5	200.8	179	5.11	47769	177
2	1% Al_2O_3	345.7	224.2	64.84	302.8	201.6	172	5.44	46840	212
3	1% Al_2O_3	341.1	211.3	61.93	301.3	200.8	183	4.84	50278	217
4	1% Al_2O_3	344.0	214.4	62.32	302.7	200.1	197	4.45	49512	181
5	1% Al_2O_3	345.3	215.7	62.48	302.7	200.4	181	4.92	48551	178
6	1% Al_2O_3	346.4	215.4	62.18	302.6	201.3	193	4.69	50995	197
7	1% Al_2O_3	336.3	216.6	64.42	302.2	201.4	184	4.92	45471	174
8	1% Al_2O_3	340.4	207.7	61.01	301.6	202.3	183	4.9	49219	181
Average		343.1	215.9	62.92	302.1	201.1	184	$\boxed{4.91}$	48579	190
Std.Dev.		3.5	5.3	1.38	0.8	0.7	8	0.29	1826	17

Run No.	Thread Compound	M/U Torque (ft-lbs)	B/O Torque (ft-lbs)	B/O to M/U Ratio	Upper Torque Curve Fit (ft-lbs)	Lower Torque Curve Fit (ft-lbs)	Points Curve Fit	Slope of Line (ft-lbs/deg)	Max Load [lbs]	Max Angle [degrees]
1	Reference	342.6	207.1	60.45	300.8	201.9	178	4.96	51533	218
2	Reference	343.9	200.4	58.27	301.7	200.8	175	4.96	53880	178
3	Reference	341.9	204.7	59.86	303.0	200.8	186	4.85	52576	221
4	Reference	346.6	205.3	59.22	301.2	201.8	182	4.71	52902	175
5	Reference	346.2	208.0	60.09	300.8	201.6	173	5.04	49578	176
6	Reference	345.7	208.2	60.23	302.2	201.5	200	4.39	51387	164
7	Reference	349.6	212.4	60.76	301.8	201.1	194	4.54	48795	166
8	Reference	348.4	211	60.56	300.3	200.3	182	4.94	48763	173
Average		345.6	207.1	59.93	301.5	201.2	184	$\boxed{4.80}$	51177	184
Std.Dev.		2.7	3.8	0.82	0.9	0.6	9	0.23	1945	23

The first set of results shown in Table V-5 above represents the test data and results for the thread compound with 1% Al_2O_3 additive. The average slope of the first 8 cycles (calibration run) with the reference compound is 4.75; the average slope of the next 8

cycles (with thread compound) is 4.91; and the average slope of the last 8 cycles using the reference compound again is 4.80.

The friction factor is then calculated to be 1.029 which indicates that the friction factor is higher than that of the reference compound. In other words, 1% Al_2O_3 additive increases the frictional properties of the reference compound by 2.9%.

Table V-6. Friction Test Result for Thread compound with 3% Al_2O_3 Additive

Run No.	Thread Compound	M/U Torque (ft-lbs)	B/O Torque (ft-lbs)	B/O to M/U Ratio	Upper Torque Curve Fit (ft-lbs)	Lower Torque Curve Fit (ft-lbs)	Points Curve Fit	Slope of Line (ft-lbs/deg)	Max Load [lbs]	Max Angle [degrees]
1	Reference	342.6	207.1	60.45	300.8	201.9	178	4.96	51533	218
2	Reference	343.9	200.4	58.27	301.7	200.8	175	4.96	53880	178
3	Reference	341.9	204.7	59.86	303.0	200.8	186	4.85	52576	221
4	Reference	346.6	205.3	59.22	301.2	201.8	182	4.71	52902	175
5	Reference	346.2	208.0	60.09	300.8	201.6	173	5.04	49578	176
6	Reference	345.7	208.2	60.23	302.2	201.5	200	4.39	51387	164
7	Reference	349.6	212.4	60.76	301.8	201.1	194	4.54	48795	166
8	Reference	348.4	211.0	60.56	300.3	200.3	182	4.94	48763	173
Average		345.6	207.1	59.93	301.5	201.2	184	4.80	51177	184
Std.Dev.		2.7	3.8	0.82	0.9	0.6	9	0.23	1945	23

Run No.	Thread Compound	M/U Torque (ft-lbs)	B/O Torque (ft-lbs)	B/O to M/U Ratio	Upper Torque Curve Fit (ft-lbs)	Lower Torque Curve Fit (ft-lbs)	Points Curve Fit	Slope of Line (ft-lbs/deg)	Max Load [lbs]	Max Angle [degrees]
1	3% Al_2O_3	343.2	218.3	63.61	302.2	200.8	186	4.75	47883	159
2	3% Al_2O_3	344.8	211.8	61.42	303.9	200.2	194	4.68	48176	166
3	3% Al_2O_3	348.3	214.8	61.68	300.4	202.3	210	4.11	48209	206
4	3% Al_2O_3	345.5	218.1	63.12	300.1	200.8	212	4.21	46155	187
5	3% Al_2O_3	342.9	210.5	61.40	301.8	201.2	195	4.69	46416	172
6	3% Al_2O_3	344.1	216.4	62.90	305.1	200.5	202	4.64	48453	184
7	3% Al_2O_3	342.0	211.9	61.96	303.0	200.7	196	4.68	46725	172
8	3% Al_2O_3	343.8	210.5	61.22	301.2	201.4	197	4.54	47491	176
Average		344.3	214.0	62.16	302.2	201.0	199	4.54	47439	178
Std.Dev.		1.9	3.3	0.91	1.7	0.6	9	0.24	892	15

Run No.	Thread Compound	M/U Torque (ft-lbs)	B/O Torque (ft-lbs)	B/O to M/U Ratio	Upper Torque Curve Fit (ft-lbs)	Lower Torque Curve Fit (ft-lbs)	Points Curve Fit	Slope of Line (ft-lbs/deg)	Max Load [lbs]	Max Angle [degrees]
1	Reference	345.0	207.7	60.20	302.3	200.4	219	4.12	49773	178
2	Reference	342.2	209.7	61.29	301.3	201.0	188	4.90	48502	187
3	Reference	334.4	208.1	62.24	301.2	201.2	183	4.97	48404	171
4	Reference	340.6	203.6	59.77	300.5	200.5	178	4.98	50718	167
5	Reference	346.0	209.1	60.41	302.5	200.0	191	4.74	50995	192
6	Reference	341.0	212.0	62.18	300.8	201.9	193	4.57	49284	183
7	Reference	343.5	208.3	60.65	300.4	200.7	198	4.65	48926	181
8	Reference	339.1	208.5	61.50	300.8	202.6	190	4.94	48388	182
Average		341.5	208.4	61.03	301.2	201.0	193	4.73	49374	180
Std.Dev.		3.7	2.4	0.92	0.8	0.9	12	0.29	1033	8

The first set of results shown in Table V-6 above represents the test data and results for the thread compound with 3% Al_2O_3 additive. The average slope of the first 8 cycles (calibration run) with the reference compound is 4.80; the average slope of the next 8

cycles (with thread compound) is 4.54; and the average slope of the last 8 cycles using the reference compound again is 4.73.

The friction factor is then calculated to be 0.952 which indicates that the friction factor is lower than that of the reference compound. In other words, 3% Al_2O_3 additive decreases the frictional properties of the reference compound by 4.8%.

It may be said, however not conclusively, that the friction performance of the thread compound with Al_2O_3 Additive decreases as the additive composition increases.

Table V-7. Friction Factor and Friction Performance of the Thread Compound

Thread Compound	S_1	S_2	S_3	Friction Factor	Frictional Performance
"1% CeO_2"	5.13	5.25	5.42	0.995	0.5% Decrease
"3% CeO_2"	5.42	5.48	5.51	1.002	0.02% Increase
"1% Y_2O_3"	5.53	5.59	5.33	1.029	2.9% Increase
"3% Y_2O_3"	5.33	5.08	4.75	1.007	0.7% Increase
"1% Al_2O_3"	4.73	4.89	4.78	1.029	2.9% Increase
"3% Al_2O_3"	4.80	4.54	4.73	0.952	4.8% Decrease

The summary of the friction factor and friction performance of the thread compounds is shown in Table V-7. It should be noted that the frictional performance is evaluated in comparison with the reference compound. 1% Y_2O_3 and 1% Al_2O_3 additives both have the best frictional performance, that is, the least COF.

Previous studies have shown that the concentration of additives within the base stock strongly influences the tribological properties of such lubrication systems [46]. In other words, there is an optimum concentration at which the coefficient of friction is at a minimum. This concept can be best explained based on the extent of nanoparticle coverage on the contacting surfaces. When the concentration is too low, the nanoparticles may not sufficiently prevent contact between the shearing surfaces. However when the concentration is too high, aggregation occurs thereby forming large clusters of nanoparticles that can serve as abrasive bodies leading to an increase in wear and friction on the mating surfaces [47]. This effect can be seen with results obtained for Al_2O_3; increasing the concentration from 1% wt. to 3% wt. caused a drastic decrease in the friction performance of the thread compound. Other factors including but not limited to, hardness, density and shape of nano-additives may influence the tribological performance of a thread compound [48]. A vivid pictorial representation of the calculated friction factor values is shown in Figure 27. Thread compounds with FF >1 have good friction performance and a low coefficient of friction.

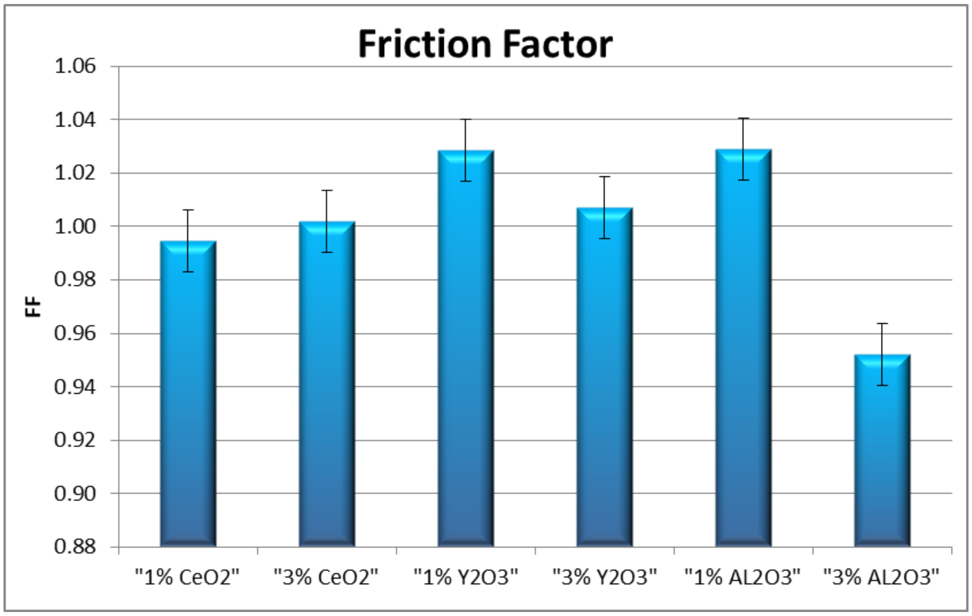

Figure 27. Friction Factor Plot

In summary, when compared with the reference compound, 1% composition of Y_2O_3 and Al_2O_3 showed better frictional performance which is responsible for higher film strength, anti-galling and anti-seize property of a thread compound.

5.2 Effects of Additive on Wear

Over the years the mechanism for anti-wear and friction reduction by additive action has been attributed to a number of concepts and various hypotheses has been put forward explaining the additive action. The 'Mending effect' proposed in [49] suggests that nano-particle additives are deposited on the friction surface and compensate for the loss of mass. The 'Ball-bearing' or 'Rolling' effect proposed in [50], suggests nano-particles polish and become inlaid between the rubbing surfaces and acts like a ball, bearing the load, thereby reducing friction and wear. In the 'Polishing effect' explained by [50], the roughness of the lubricating surface is reduced by the abrasive property of nano-additives. Figure 28 depicts the various hypotheses for additive action in surface wear reduction. The ‘Protective effect’ as the name suggests, entails the formation of a protective layer. Nano-additives react with the metal substrate to generate chemical tribofilms with a layered structure and excellent tribological properties [51]. In this research, based on above discussion, there are two possibilities. The first is that oxides were directly deposited on the steel surface forming a protection coating. The second is that tribochemical reactions resulted in some reactive products enhancing the protection. Future research will be conducted to prove the mechanisms.

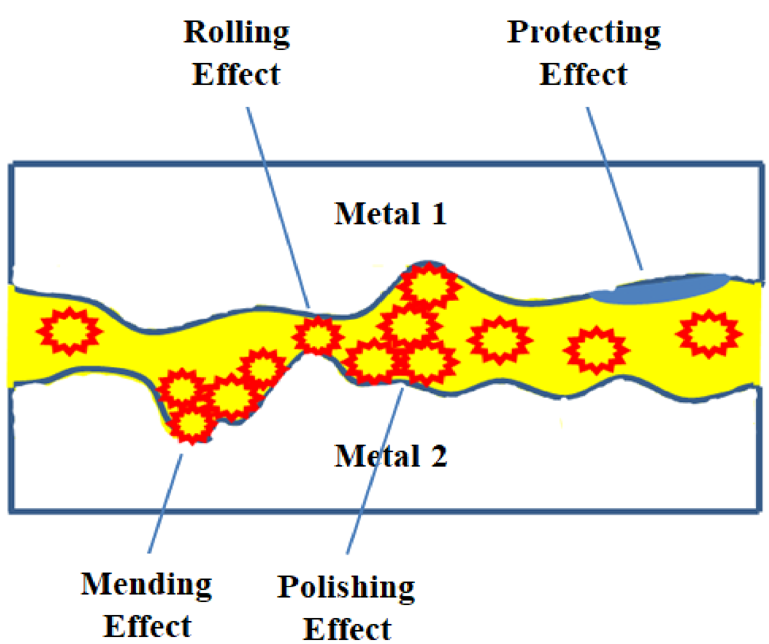

Figure 28. Additive Action for Wear Reduction [52]

CHAPTER VI

CONCLUSION AND FUTURE RECOMMENDATIONS

6.1 Conclusions

This research studied the effectiveness of selected metal oxides (CeO_2, Y_2O_3 and Al_2O_3) as additives in semi-solid lubricants. The goal to evaluate a novel grease with new additives with improved corrosion and galling resistance has been achieved. Two different experiments were conducted: The corrosion test and the API RP 7A1 thread compound test.

Compared with base grease, all additives showed significant improvement in corrosion protection. Al_2O_3 additive in 1% and 3% composition showed the highest improvement in corrosion prevention.

1% Al_2O_3 had approximately a 90% improvement in corrosion protection.

3% Al_2O_3 had approximately a 98% improvement in corrosion protection.

Also, yttria showed a greater effect than ceria in inhibiting corrosion.

The corrosion study has shown that the proposed additives used in this research can bring about a significant improvement in the corrosion protective property of lubricants. Thereby extending the service life of equipment in corrosive service.

There are 3 main findings from the galling tests:

1) 1% and 3% weight concentration of CeO_2 had no significant effect on improving the frictional performance of the thread compound.
2) 1% wt. Y_2O_3 had a 2.9% increase in the frictional performance. Increasing the concentration to 3% lead to a reduction in frictional performance.
3) 1% wt. Al_2O_3 had a 2.9% increase in the frictional performance. Increasing the concentration to 3% had a detrimental effect on the frictional performance.

The galling tests have shown that Y_2O_3 and Al_2O_3 additives added in the right composition increases the frictional and anti-galling performance of thread compounds used in a wide range of high contact stress applications.

From the findings above, it may be concluded that the optimization is possible for corrosion prevention and reducing friction. Adding nanoparticles into a thread compound is a novel approach that opens up new revenues for future directions.

6.2 Future Recommendations

Based on results found in this research, the below actions and works are suggested:

1) Investigation of the effect of elevated temperatures and pressure.

This is important in order to understand the effectiveness of the grease additives under High Temperature and High Pressure (HPHT) conditions.

2) Shapes and Structure of nanoparticles.

Studies have also shown that the shape and structure of nanoparticle films have a great influence on their adhesion and frictional properties. An investigation of the effect of shape and structure of CeO_2, Y_2O_3 and Al_2O_3 additives could prove beneficial.

3) Evaluation of tribo-chemical reaction and chemical analysis

The investigation into the nature of chemical reactions occurring at the surface would provide a better understanding into the mechanism of additive action in wear and corrosion protection.

REFERENCES

[1] G. Labouratories, "Cost of Corrosion Annually in the US over $1 Trillion," Apr 2015. [Online]. Available: http://www.g2mtlabs.com/corrosion/cost-of-corrosion/.

[2] A. International, "The Effects and Economic Impact of Corrosion," *Corrosion: Understanding the Basics*, 2000.

[3] A. A. Oyelami BO, "Mathematical modelling: An application to corrosion in a petroleum industry," in *NMC Proceedings Workshop on Environment.*, Abuja, Nigeria.

[4] Saylor, "Corrosion," Saylor, [Online]. Available: https://saylordotorg.github.io/text_general-chemistry-principles-patterns-and-applications-v1.0/s23-06-corrosion.html. [Accessed 05 May 2017].

[5] W. E. Corbin D, "New technology for real-time corrosion detection.," in *Tri-service corrosion conference*, USA, 2007.

[6] M. G. Fontana, Corrosion Engineering, McGraw-Hill, 1987.

[7] L. R. Rudnick, Lubricant Additives Chemistry and Applications, CRC Press, 2003.

[8] www.nace.org, "NACE International," [Online]. Available: https://www.nace.org/uploadedFiles/Corrosion_Central/Corrosion Control and Environmental Protection.pdf. [Accessed June 2017].

[9] "Thread Galling," Bolt Depot, [Online]. Available: https://www.boltdepot.com/fastener-information/materials-and-grades/Thread-galling.aspx. [Accessed 17 June 2017].

[10] M. G. Donald A. Oldiges, "Anti-seize thread compound". US Patent WO1996034931 A1, 7 November 1996.

[11] N. Jacobs, "Metal-free lubricant composition containing graphite for use in threaded connections". US Patent 5,180,509, 1993.

[12] ASTM, "ASTM D288 - Definitions of Terms Relating to Petroleum," ASTM

International (ASTM), 1961.

[13] J. Wright, "Grease Basics," Noria Company, May 2008. [Online]. Available: http://machinerylubrication.com/Read/1352/grease-basics.

[14] M. Johnson, "Selecting the correct lubricant," *Tribology & Lubrication Technology,* p. 31, 2008.

[15] Lubricants intelligence network, [Online]. Available: http://www.lube-info.com/2016/0805/4572.html. [Accessed 25 May 2017].

[16] P. Anthony Grossi, "All About Lubricant Additives," Power, 01 August 2016. [Online]. Available: http://www.powermag.com/all-about-lubricant-additives/.

[17] D. N. Canter, "Use of antioxidants in automotive lubricants," September 2008. [Online]. Available: www.stle.org.

[18] Lashkhi, V.L., Grishin, N.N., Fuks, I.G.,N. A. Mityagin, "Principles of corrosion inhibitor selection for lubricating greases," in *Chem Technol Fuels Oils*, Kluwer Academic Publishers-Plenum Publishers, 1992, p. 450–453.

[19] IEEE GlobalSpec, "Rust and Corrosion Inhibiting Fluids," Engineering 360, [Online]. Available: http://www.globalspec.com/. [Accessed 25 April 2017].

[20] Bennett Fitch, "The Importance of Lubricant Film Strength," Noria Corporation, [Online]. Available: http://www.machinerylubrication.com/Read/30835/lubricant-film-strength. [Accessed 15 July 2017].

[21] "What are Friction Modifiers?," [Online]. Available: http://www.machinerylubrication.com/Read/28815/what-are-friction-modifiers. [Accessed 07 July 2017].

[22] "Ceric Oxide," Pubchem, 27 March 2005. [Online]. Available: https://pubchem.ncbi.nlm.nih.gov/compound/Ceric_oxide#section=Industry-Uses.

[23] Adnan Younis, Dewei Chu and Sean Li, *Cerium Oxide Nanostructures and their Applications,* Intech, 2016.

[24] A. Trovarelli, Catalysis by Ceria and Related Materials, London: Imperial College

Press, 2002.

[25] Reade, "Cerium Oxide Powder (CeO2)," Reade, [Online]. Available: http://www.reade.com/products/cerium-oxide-powder-ceo2. [Accessed 04 July 2017].

[26] W. M. Haynes, Handbook of Chemistry and Physics, CRC Press, 2015.

[27] Rajendra N. Mitra, Miles J. Merwin, Zongchao Han, Shannon M. Conley, Muayyad R. Al-Ubaidi, and Muna I. Naash, "Yttrium oxide nanoparticles prevent photoreceptor death in a light-damage model of retinal degeneration," *PubMed Central*, pp. 140-148, 2014.

[28] Milind S Hatwalne, "Free radical scavengers in anaesthesiology and critical care," *Indian Journal of Anaesthesia*, pp. 227-233, 2012.

[29] Skyworks Solutions, Inc., "Yttrium Oxide (Y2O3)," [Online]. Available: http://www.skyworksinc.com/uploads/documents/yttriumoxide.pdf. [Accessed 06 08 2017].

[30] K. Strecker, S. Ribeiro, M.-J. Hoffman, M. J. Bondioli, "Mechanical properties of SiC ceramics sintered with AlN-Y2O3 additives," *Materials Research*, vol. 3, no. 18, pp. 525-529, 2015.

[31] National Center for Biotechnology Information, "PubChem Compound Database; CID=9989226," [Online]. Available: https://pubchem.ncbi.nlm.nih.gov/compound/9989226. [Accessed 22 June 2017].

[32] D. Gualtieri, "Transparent Aluminum," [Online]. Available: http://tikalon.com/blog/blog.php?article=2015/transparent_aluminum. [Accessed 22 June 2017].

[33] D. Gualtieri, "Transparent Aluminum," tikalon, 4 June 2015. [Online]. Available: http://tikalon.com/blog/blog.php?article=2015/transparent_aluminum.

[34] Accuratus, "Aluminum Oxide, Al2O3 Ceramic Properties," 2013. [Online]. Available: http://accuratus.com/alumox.html. [Accessed 22 June 2017].

[35] CeramTec, "Oxide Ceramics – Aluminum Oxide (Al2O3)," [Online]. Available: https://www.ceramtec.com/ceramic-materials/aluminum-oxide/. [Accessed 22 June

2017].

[36] API RP 7A1, "Recommended Practice for Testing of Thread Compound for Rotary Shouldered Connections," 1992.

[37] "Special Metals," [Online]. Available: www.specialmetals.com/assets/smc/documents/inconel_alloy_718.pdf. [Accessed 20 June 2017].

[38] "Nickel Alloy 718/ Inconel 718," Aircraft Materials, [Online]. Available: https://www.aircraftmaterials.com/data/nickel/718.html. [Accessed 22 oct 2017].

[39] B. R. L. V. D.G. Thakur, "A study on the surface integrity aspects of superalloy Inconel 718 under minimum quantity lubrication in high speed turning," *International Journal of Materials and Structural Integrity,* vol. 5, no. 1, 2011.

[40] M.S. Al-Otaibi, A.M. Al-Mayouf, M. Khan, A.A. Mousa, S.A. Al-Mazroa, H.Z. Alkhathlan, "Corrosion inhibitory action of some plant extracts on the corrosion of mild steel in acidic media," *Arabian Journal of Chemistry,* vol. 7, no. 3, pp. 340-346, 2014.

[41] M. Costello, "Corrosion Inhibitors and Rust Preventatives," in *Lubricant Additives,* New York, NY, Marcel Dekker, Inc.:, 2009, pp. 421-444.

[42] Camila G. Dariva and Alexandre F. Galio, "Corrosion Inhibitors – Principles, Mechanisms and," no. DOI: 10.5772/57255 .

[43] NCSU, "SOLUBILITY PRODUCT CONSTANTS," [Online]. Available: http://www4.ncsu.edu/~franzen/public_html/CH201/data/Solubility_Product_Constants.pdf. [Accessed 9 September 2017].

[44] P. F. Alessandro Trovarelli, in *Catalysis by Ceria and Related Materials,* 2013, p. 846.

[45] Bestolife, "Friction Factor," Bestolife Premium Compounds, [Online]. Available: https://www.bestolife.com/pages/friction-factor. [Accessed 23 June 2017].

[46] Andrei Khurshudov∗, Robert J. Waltman, "Tribology challenges of modern magnetic hard disk drives," *Wear,* no. 251, p. 1124–1132, 2001.

[47] Sunqing Qiu, Zhongrong Zhou, Junxiu Dong, Guoxu Chen, "Preparation of Ni nanoparticles and evaluation of their tribological performance as potential additives in oils," *Journal of Tribology,* vol. 3, no. 123, pp. 441-443, 2001.

[48] S. K. T. Lesniewski, "The effect of ball hardness on four-ball wear test results," *Wear,* vol. 264, no. 7-8, pp. 662-670, 2008.

[49] G. Liu, X. Li, B.Qin, D.Xing, Y. Guo, and R. Fan, "Investigation of the mending effect and mechanism of copper nano-particles on a tribologically stressed surface," *Tribology Letters,* vol. 17, no. 4, p. 961–966, 2004.

[50] X. Tao, Z. Jiazheng, and X. Kang, "The ball-bearing effect of diamond nanoparticles as an oil additive," *Journal of Physics,* vol. 29, no. 11, pp. 2932-2937, 1996.

[51] M. Ratoi, V. B. Niste, and J. Zekonyte, "WS2 nanoparticles—potential replacement for ZDDP and friction modifier additives," *RSC Advances,* vol. 4, no. 41, p. 21238–21245, 2014.

[52] Tianyi Sui, Baoyu Song, Feng Zhang, and Qingxiang Yang, "Effect of Particle Size and Ligand on the Tribological," *Journal of Nanomaterials Properties of Amino Functionalized Hairy Silica Nanoparticles as an Additive to Polyalphaolefin,* 2015.

[53] P. Kofstad, Nonstoichiometry, Diffusion, and Electrical Conductivity in Binary Metal Oxides, New York: Wiley Interscience, 1972.

[54] B. Kilbourn, "yttria," *Encyclopedia of Materials Science and Engineering,* vol. 7, pp. 5509-5510, 1986.

[55] M. Stern and A. L. Geary, "Electrochemical Polarization I. A Theoretical Analysis of the Shape of Polarization Curves," *Journal of the Electrochemical Society,* vol. 104, no. 1, pp. 56-63, 1957.

[56] J. M. Dowding, "CeO2 NPS act as a Unique Catalyst and Scavenge ·NO AND ONOO- and Decrease RNS in Vitro and in Vivo," 2012.

[57] Pierre R. Roberge, Handbook of corrosion engineering, New York: McGraw-Hill, 2000.

[58] He, Xingliang, "Synthesis, Characterization, Properties, and Tribological Performance of 2D Nanomaterials," 2014.

[59] R. LIU, D.Y. LI, "Effects of yttrium and cerium additives in lubricants on corrosive wear of stainless steel 304 and Al alloy 6061," *Journal of Material Science,* no. 35, pp. 633-641, 2000.